Canadian Science Publishing | Canadian Journal of Earth Sciences

Allochthonous sources of iodine and organic carbon in an Eastern Ontario aquifer

Journal:	*Canadian Journal of Earth Sciences*
Manuscript ID	cjes-2018-0082.R1
Manuscript Type:	Article
Date Submitted by the Author:	23-Jun-2018
Complete List of Authors:	Lemieux, Alexander; University of Ottawa, Science Hamilton, Stewart; Ontario Geological Survey Clark, Ian; Dept of Earth Sciences,
Keyword:	Champlain Sea, Iodine-129, Radiocarbon, Glacial meltwaters, Iodine enrichment
Is the invited manuscript for consideration in a Special Issue? :	Advances in low temperature geochemistry diagenesis seawater and climate: A tribute to Jan Veizer

Allochthonous sources of iodine and organic carbon in an Eastern Ontario aquifer

Lemieux, A.J.[1] (alemi071@uottawa.ca), Hamilton, S.M.[2] (stew.hamilton@ontario.ca), and Clark, I.D.[1] (idclark@uottawa.ca)

[1]*Faculty of Earth and Environmental Sciences, University of Ottawa, Ottawa, Ontario, Canada*

[2]*Ontario Geological Survey, Sudbury, Ontario, Canada*

Corresponding author: Alexander Lemieux, alemi071@uottawa.ca, 613-558-6608. 25 Templeton Street, Ottawa, Ontario, Canada, K1N 6N5.

Abstract

Regional geochemical characterization of groundwaters in a bedrock aquifer in the Ottawa – St. Lawrence Lowlands of Eastern Ontario has identified an iodine (I) anomaly, with values regularly exceeding 150 µg/L, and a maximum observed concentration of 10 812 µg/L. The spatial distribution, enrichment mechanisms, and sources of I and organic matter were investigated using geochemical and isotopic data. High-I groundwaters (> 150 µg/L) are prevalent in Na-Cl type groundwaters at low bedrock elevations in areas overlain by thick layers of glacial sediments. I is thought to be linked to massive muds in the glacial sediments overlying the aquifer, deposited during the postglacial incursion of the Champlain Sea 10 – 12 ka BP. Principal component analysis of I and 18 other chemical parameters revealed correlations between I, salinity, and indicators of microbial oxidation of organic matter, suggesting that the intrusion of saline porewaters affected by decomposition of organic matter such as marine phytoplankton in the massive muds is the dominant process controlling I enrichment in groundwater. $^{129}I/^{127}I$ ratios in the pre-modern waters vary between near marine values of 150×10^{-14} and 5×10^{-14}, demonstrating that older, allochthonous I derived from the surrounding Paleozoic sedimentary terrain also contributed to the I pool in the Champlain Sea basin. ^{14}C ages and $\delta^{13}C$ signatures for dissolved organic carbon (DOC) in groundwater and disseminated organic carbon within the glaciomarine muds highlight an allochthonous source of terrestrial organic carbon predating the Champlain Sea incursion, likely transported in tandem with I to the Champlain Sea basin via glacial meltwaters.

Keywords: Champlain Sea, Iodine-129, Radiocarbon, Glacial meltwaters, Iodine enrichment

Introduction

Geochemical analysis of shallow groundwaters (<200 mBGS) sampled from residential and monitoring wells in the central St-Lawrence lowlands region in Eastern Ontario by the Ontario Geological Survey (OGS) and South Nation Conservation Authority (SNCA) during the summers of 2012, 2013, and 2015 revealed problem areas with anomalously high concentrations of iodine (I) as iodide (I^-) up to 10 812 µg/L (OGS, 2016). I is an essential element for synthesis of thyroid hormones in the human body and an excess or deficiency can be harmful. Chronically high I intake above the proposed upper limit of 1 000 µg/day for adults can increase the risk of hyperthyroidism and goiter (WHO, 2007), and I-rich drinking water in China was shown to contribute to increased incidences of these health issues (Andersen et al., 2008). In China, a threshold I concentration of 150 µg/L in groundwater is used to define areas at risk of excessive I intake (China Ministry of Health, 2003), a guideline which is regularly surpassed in the study area. Although there is currently no drinking water limit for I in Canada (Health Canada, 2017) it is estimated that 15% of the Canadian population between the ages of 3 – 79 have an excessive I intake (Stats Canada, 2013) based on optimal urine concentrations of I required for nutritional sufficiency defined by the World Health Organization (WHO, 2007). Additionally, levels of I in milk from Ontario dairy herds exhibit greater average I concentrations of 345 µg/kg compared to a Canadian average of 304 µg/kg (Castro et al., 2010). In Eastern and Southern Ontario, this phenomenon is thought to be linked to consumption of high-I groundwater by dairy cows (Rogerson et al., 2016).

The phenomenon of I enrichment in groundwater affects many regions in the world including Japan (Kashiwagi et al., 2006; Togo et al., 2016), Denmark (Andersen et al., 2002; Voutchkova et al., 2014; Voutchkova et al., 2017), Canada (Fabryka-Martin et al., 1991;

Hamilton et al., 2015), and China (Zhang et al., 2010; Li et al., 2013; Zhang et al., 2013; Duan et al., 2016). In these areas, decomposition of organic matter within marine sediments is typically one of the mechanisms invoked to explain I enrichment in groundwater (Kashiwagi et al., 2006; Li et al., 2013; Zhang et al., 2013; Hamilton et al., 2015; Duan et al., 2016). In marine or estuarine environments, I is concentrated into phytoplankton or other plants (Moisan et al., 1994) and correlates with organic matter in marine sediments (Fuge and Johnson, 1986; Malcolm and Price, 1984). The relative I content of sedimentary reservoirs decreases from recent marine sediments (5 – 200 mg/kg) to soils (2 – 15 mg/kg), shales/carbonates (2.3 – 2.7 mg/kg), sandstones (0.8 mg/kg) and finally igneous/metamorphic rocks (0.24 – 0.30 mg/kg), based on values reported in Fuge and Johnson (1986). The St-Lawrence lowlands of Eastern Ontario and southwestern Québec are characterized by thick layers of glaciomarine muds deposited during a post-glacial marine incursion referred to as the Champlain Sea, which occurred from 12 – 10 ka BP (see Geology and Hydrogeology section). It is expected that high I groundwaters in Eastern Ontario are due to the leaching of porewater enriched in I from the decomposition of organic matter within glaciomarine muds. The prevalence of high-I groundwater in Eastern Ontario highlights the need for a better understanding of the factors controlling the spatial variability and release of I, as well as the sources of I and organic carbon in the glaciomarine muds. The objectives of this study were 1) to characterize the hydrogeochemical environments in which naturally high I groundwater (> 150 µg/L) is prevalent, 2) identify the link between I and other geochemical parameters using multivariate statistical analysis to evaluate which factors influence I concentrations and 3) apply a stable and radioisotopic dataset to trace the sources of organic carbon and I in the studied aquifer, as they are poorly understood.

Study Area

The study area is situated in the central St. Lawrence Lowlands region of Eastern Ontario at an average elevation of 70 mASL and lies 50 kilometres east of the City of Ottawa, along the southern shore of the Ottawa River (see Figure 1). With a combined population of 32 000 people in 2011 (Stats Canada, 2016), the main study area covers an area close to 1 500 km^2 and is comprised of two jurisdictions: The Township of Alfred-Plantagenet and the City of Clarence-Rockland. These, in turn, are within the United Counties of Prescott and Russell. Most villages within the study area are serviced by water treatment plants that pump water from the Ottawa River. Outside of the serviced areas, groundwater is the primary source of drinking water.

Geology and Hydrogeology

The geology of the study area (Figure 1c) consists of Precambrian basement of the Canadian Shield overlain by Paleozoic sedimentary rocks including sandstones (Covey Hill, Nepean, March, and Rockcliffe formations) as well as interbedded shales (Billings, Carlsbad and Queenston formations) and carbonates (Oxford, Gull River, Bobcaygeon, Verulam, and Lindsay formations), as per Armstrong and Dodge (2007). The most recent Quaternary glaciation (Wisconsinian) resulted in the deposition of tills, subglacial outwash deposits (primarily sands), and glaciomarine sediments, comprised of glaciomarine muds and nearshore sands, atop the bedrock units. In the study area, sandy silt tills from the erosion of carbonates are the most prevalent, due to the abundance of localized carbonaceous sedimentary rocks. The retreat of the Laurentide ice sheet from the region at approximately 12 ka BP uncovered an isostatically depressed landmass which resulted in a marine incursion from the Gulf of St-Lawrence, forming the Champlain Sea, which was present for approximately 2 000 years (Barnett, 1992). The depositional sequence of Champlain Sea muds in the study area was described by Gadd (1986),

who reported three mud units (from oldest to youngest): basal rhythmites, massive muds, and red-and-grey stratified mud. The entire sequence of mud and overlying nearshore sands ("glaciomarine sediments") was interpreted to be produced by deltaic offlap during regression of the Champlain Sea. Massive muds are the most abundant and widespread deposits and have an average thickness of approximately 10 meters with a maximum observed thickness of 90 meters in the studied area (Charron, 1975). Locally, the highest observed porewater salinities are observed in the massive muds and are thought to reflect the salinity of the Champlain Sea (Torrance, 1988). The glaciomarine muds overlie till and subglacial outwash sands in most areas, with the exception of topographic high areas, where till or exposed bedrock is found at the surface. The muds reach their maximum thicknesses in topographically low areas and typically exhibit an organic carbon content ranging from 0.4-1 wt.% (Donovan and Lajoie, 1979). Deposits containing significant proportions of organic matter that predate that the till are also present in the central St. Lawrence Lowlands, although there is no evidence from local well logs of the presence of these deposits in the studied area. These deposits are referred to as the St. Pierre sediment, deposited during the Les Becquets interstadial period that occurred from the late Sangamonian to Early Wisconsinian, between 60 – 75 ka BP (Ochietti, 1989). Peat and organic-rich sand from this unit in a quarry ~50 km east of the studied area at Pointe-Fortune, Québec, were found by radiocarbon (^{14}C) dating to be older than 42 ka BP (Veillette and Nixon, 1984).

The principal hydrostratigraphic unit of the St-Lawrence lowlands is described as an interface aquifer (Cloutier et al., 2006; Montcoudiol et al., 2015), comprised of a layer of till, subglacial outwash sands and highly fractured bedrock separating the overlying muds from the moderately fractured Paleozoic bedrock underneath. Meteoric water recharges the system in topographically high areas where there is little to no mud cover and flows preferentially in the

upper bedrock beneath the mud via the interface flow system to topographically low areas. Depressions in the bedrock surface throughout the study area represent the final feature of the flow system. These depressions contain remnant Champlain Sea waters which are confined by a thick layer of overlying mud, and underneath by low-permeability bedrock. The system can be divided into three components: an unconfined recharge area, a semi-confined transition area, and a confined lowland area, as shown by the conceptual model in Figure 2. Charron (1975) noted that groundwater flow is controlled by bedrock topography in the study area due to the fact that the permeable interface zone is located at the contact between bedrock and surficial sediment deposits. Groundwater residence times in the confined lowland areas typically exceed 5 ka (Montcoudiol et al., 2015).

Although flow regimes in the study area are predominantly horizontal as they travel through the continuous layer that constitutes the interface aquifer, solute diffusion from the low-permeability muds is non-negligible and can have profound impacts on water geochemistry, as demonstrated by Cloutier et al. (2006). Additionally, in a hydrogeological study of the St-Lawrence River Valley, Chapuis and Saucier (2013) concluded that the Champlain Sea muds are underdrained by groundwater ("leaky") aquifers, which collect small amounts of vertically seeping porewaters.

Methods and Theory

Previously visited sites from sampling campaigns (n = 139) conducted during the summers of 2012 (Freckelton and Hamilton, 2012), 2013 (Morton et al., 2013), and 2015 (Di Iorio et al., 2015) as part of the Ontario Ambient Groundwater Geochemistry Program (OAGGP) were screened based on their respective I content and revisited in the summer of 2016.

Additionally, new sites were visited in areas with historically high-I groundwaters. In total, 61 sites were visited during the summer of 2016, 169 sites were sampled in the study area from 2012 – 2016 and iodide concentrations varied from 2 – 10 812 µg/L, with an average of 646 µg/L (OGS, 2016). 47% (n = 79) of the sites visited exhibited I concentrations exceeding 150 µg/L. The purpose of returning to sampling sites was threefold: to homogenize available hydrogeochemical datasets, collect samples from sites representing the full range of I concentrations in the study area, and to collect samples to be analyzed for ^{129}I and $^{14}C/\delta^{13}C$ of dissolved inorganic/organic carbon (DIC/DOC), which had not been done in previous sampling iterations. Additionally, two glaciomarine mud samples were collected at an approximate depth of six mBGS for ^{14}C and $\delta^{13}C$ analysis of disseminated organic matter during the 2016 campaign. Groundwater and mud sample locations are shown in Figure 1.

Sampling

The pH, temperature, dissolved oxygen, conductivity, oxidation-reduction potential, H_2S and alkalinity of water samples were measured in the field. Wells were purged until the stabilization of field parameters, typically when temperature variations were within a range of ±0.1˚C, at which point samples were collected in high-density polyethylene (HDPE) bottles and stored at 4˚C until analysis of major, minor, and trace constituents for a total of 65 parameters, in addition to DIC, DOC, $\delta^{13}C_{DIC/DOC}$, ^{129}I, and enriched tritium (^{3}H). Samples to be analyzed for major, minor, and trace constituents as well as DIC and DOC were filtered using a 0.45 µm polyvinylidene fluoride filter. At sites where there was significant exsolution of gas in the form of free bubbles during pumping (n = 19) gas samples to be analyzed for ^{14}C of methane (CH_4) and $\delta^{13}C_{CH4}$ were collected in using the inverted bottle method, and groundwater samples to be analyzed for $^{14}C_{DIC/DOC}$ were filtered using a 0.45 µm polyethersulfone filter. Gas and water

samples for ^{14}C analysis were collected in borosilicate bottles with a plastic cap and butyl septum to minimize atmospheric exchange. Data collected for CH_4 are not relevant to the scope of this study and are thus not presented in the text. More information regarding sampling methodology and site selection can be found in Lemieux et al. (2016).

Analytical Methods

Major, minor and trace cation and anion concentrations, including Ca, Mg, Na, K, Fe, Al, Mn, Cl, Br, and SO_4 were measured at Geoscience Laboratories (GeoLabs) in Sudbury, Ontario, Canada. Cations were analyzed by both inductively coupled plasma mass spectrometry (ICP-MS) using a Perkin Elmer Elan 9000 ICP-MS and inductively coupled plasma atomic emission spectrometry (ICP-AES) using a Teledyne Leeman Laboratories Prodigy ICP AES Radial View instrument. Anions were analyzed by Ion Chromatography (IC), using a dual-pump system ion chromatograph, Dionex model ICS-3000. Overall method precision was determined with field and laboratory duplicate pairs using the method of Thompson and Howarth (1978).

$NO_2 + NO_3$ and NH_3/NH_4 were analyzed by SGS analytical laboratories in Lakefield, Ontario, Canada within seven days of collection. Nitrate (NO_3^-) and nitrite (NO_2^-) were analyzed using a Dionex Ion Chromatograph and reported as ppm N. Ammonia (NH_3) and Ammonium (NH_4^+) were analyzed using a Skalar Segmented Flow Autoanalyzer.

Within the range of pH and oxidative-reductive conditions found at the Earth's surface or within its oceans, I is present in three oxidation states: -1(iodide, I^-), +5 (iodate, IO_3^-), and 0 (gaseous iodine, I_2). The Eh-pH diagram for I speciation is presented in Figure 3 (also known as a Pourbaix diagram), along with Eh-pH values for collected groundwater samples in the study area. The conditions indicated in the diagram suggest that all I in the present groundwater system would be present as iodide (I^-). I concentrations as I^- were measured within five days of sample

collection using a Thermo Scientific™ Orion™ 9453BN Iodide Electrode connected and operated through an Orion™ Star A324 portable meter. The meter was calibrated to 10 ppb I^-, 1000 ppb I^- and 10 000 ppb I^-. Prior to measurement, the water filling the neck of each 60 mL bottle was discarded, and 1 mL of ionic strength adjuster and a micro-magnetic stir bar were added. The meter was inserted into the sample bottle, placed over a magnetic stirring plate and a measurement was recorded after the meter automatically indicated the probe had stabilized.

C isotopes of dissolved species in water and disseminated organic matter within collected mud samples ($\delta^{13}C$) were analyzed at the G.G. Hatch Stable Isotope laboratory at the University of Ottawa. Groundwater samples were first run on an OI Analytical analyzer for total inorganic carbon and total organic carbon (TIC-TOC) (Aurora Model 1030) with a model 1088 autosampler to determine concentrations for organic/inorganic carbon (in ppm C). The TIC-TOC analyzer was interfaced to a Finnigan MAT Delta plus XP IRMS for analysis by continuous flow. Analytical precision is ±2% for quantitative analysis, and ±0.2‰ for $\delta^{13}C$. $\delta^{13}C$ values are reported relative to the Vienna Pee Dee Belemnite (VPDB) standard.

For analysis of the collected glaciomarine muds, the samples were flash combusted at 1800˚C in an Elementar VarioEL Cube Elemental Analyser, and generated gases (CO_2, N_2, SO_2, H_2O) were subsequently quantitatively measured with a thermal conductivity detector (TCD) with a precision of ±0.1%. The $\delta^{13}C$ isotopic composition of released CO_2 was measured using a DeltaPlus Advantage isotope ratio mass spectrometer, which was coupled to the EA with a ConFlo III interface. Precision of the isotopic analyses was ±0.2‰.

Dissolved inorganic carbon (DIC), dissolved organic carbon (DOC), and disseminated organic carbon in the muds were prepared for ^{14}C analysis at the Andre E. Lalonde AMS Laboratories at the University of Ottawa using techniques outlined in Crann et al. (2017). Results

are reported in percent modern carbon (pMC) relative to the Ox-II modern carbon standard (NIST SRM 4990C) and are normalized to a $\delta^{13}C$ value of -25‰ (relative to VPDB). ^{14}C ages are calculated as -8033ln(pMC) and reported in ^{14}C years BP (BP = AD 1950).

A carrier-addition method described by Herod (2015) was used to extract I during a series of redox transformations for ^{129}I analysis at the Andre E. Lalonde AMS laboratory using an HVE 3MV Tandetron, Measurements were normalized with respect to the ISO-6II reference material for which $^{129}I/^{127}I = (5.72 \pm 0.08) \times 10^{-12}$, by calibration with the NIST 3230 I and II standard reference material. Results are reported as $^{129}I/^{127}I$ ratio x 10^{-14}. Standard deviations for $^{129}I/^{127}I$ ratios of individual analyses varied between ±0.1 to 2.6.

Enriched ^{3}H analysis was performed at the University of Waterloo Environmental Isotope Laboratory. ^{3}H values were measured by electrolytic enrichment (≥15x) with liquid scintillation counting (LSC). Samples with a specific conductivity exceeding 5000 µs/cm were subjected to azeotropic distillation. Results are reported in tritium units (TU), where 1 TU = 1 T per $10^{18}H$, with a detection limit of 0.8 TU and a precision of ±0.5 TU.

Data Availability

The full hydrogeochemical dataset containing major, minor, and trace ion concentrations and station data for all field seasons (2012, 2013, 2015, 2016) is publicly available for download using the OGSEarth application from the Ontario Geological Survey website (https://www.mndm.gov.on.ca/en/mines-and-minerals/applications/ogsearth), as part of the Ontario Ambient Groundwater Geochemistry Program (OAGGP). Isotopic data (^{129}I, ^{3}H, and $^{14}C/\delta^{13}C$ of DIC and DOC) is presented in the text.

Principal Component Analysis and Data Preparation

Principal Component Analysis (PCA) has previously been used to understand the correlation between chemical variables and I and to infer the geochemical processes responsible for its spatial variation in groundwater in Denmark (Voutchkova et al., 2014) and China (Zhang et al., 2013; Duan et al., 2016), and was applied to the current dataset using version 3.3.1 of the programming language R (R, 2016). The procedure used to prepare the dataset for analysis resembles that of Cloutier et al. (2008) and Montcoudiol et al. (2015). Parameters were excluded based on recommendations from Güler et al. (2002). For example, chemical parameters that were additive, redundant, measured in the field, exhibited little regional variation, and that had many (over 15% of samples) values below the detection limit or no result available were excluded. Samples exhibiting a charge balance error > ± 10% were excluded from analysis. From the current dataset, 19 chemical parameters were retained for analysis: B, Ba, Br, Ca, Cl, DOC, F, Fe HCO_3, I, K, Li, Mg, Mn, Na, NH_4, Si, SO_4 and Sr. In total, the results from 146 of the 169 collected samples were retained for PCA. Eight samples were rejected upon the basis of charge balance error, eleven for multiple missing values or values below detection limit, and four were rejected because they exhibited evidence of water treatment and thus did not represent raw groundwater. In instances where the value of a retained chemical parameter for a given sample was below the detection limit, this value was replaced with 55% the detection limit (Sanford et al., 1993). All variables were log-transformed, apart from HCO_3, which exhibited normal distribution (skewness <1). The variables were standardized, resulting in a new set of values (Z_i) with a mean of 0, measured in units of standard deviation. Six principal components were retained based on the Kaiser criterion (Eigenvalue > 1), and a Varimax normalized rotation was applied to maximize perceived variance between the retained components.

Theory: ^{129}I

There are two isotopes of I in the natural environment: stable ^{127}I and ^{129}I, the only long-lived radioactive isotope, which has a decay half-life of 15.7 Ma. ^{129}I is produced through three different pathways: cosmic spallation of Xe atoms in the upper atmosphere ("cosmogenic"), from the spontaneous fission of ^{238}U in the subsurface ("geogenic"), from fallout during past atmospheric testing of nuclear bombs and through releases from nuclear fuel reprocessing ("anthropogenic"). The long half-life, in conjunction with its long residence time in the marine environment (40 000 years), would suggest that the pre-anthropogenic $^{129}I/^{127}I$ ratio would have been fairly constant, and has been estimated to be between $30 – 300 \times 10^{-14}$ based on fissiogenic and atmospheric inputs (Fabryka-Martin et al., 1985), and $\sim 150 \times 10^{-14}$ based on measurements of recent marine sediments with no anthropogenic contamination (Fehn, 2000). Given the long half-life of ^{129}I (15.7 Ma) and the timing of the postglacial marine incursion (12 ka BP), it is expected that I derived from seawater during the Champlain Sea incursion would exhibit a $^{129}I/^{127}I$ ratio close to 150×10^{-14}.

In geological formations exceeding 100 Mya in age, the quantity of ^{129}I typically remains constant because the production rate from ^{238}U fission in the host rock is equal to the decay rate, which is referred to as secular equilibrium. Fabryka-Martin et al. (1985) calculated the estimated secular equilibrium $^{129}I/^{127}I$ ratios for I in groundwater derived from different bedrock types, which depend largely on the ^{129}I production rate (a function of the fractional ^{238}U concentration in the rock) and the leaching efficiency of produced ^{129}I from the host formation. Estimated groundwater $^{129}I/^{127}I$ values for samples derived from geological units relevant to the studied area vary from approximately 3×10^{-14} for limestones, 13×10^{-14} for clay shales, 63×10^{-14} for black shales, 320×10^{-14} for sandstones and 470×10^{-14} for crystalline granite. $^{129}I/^{127}I$ ratios for

modern surface and recharge waters in North America are much higher, estimated to be on the order of 10^{-8} (Rao and Fehn, 1999; Rädlinger and Heumann, 2000) due to significant ^{129}I releases associated with nuclear activities.

Results

Spatial distribution of I

Univariate analysis was conducted on the retained 146 samples after data preparation to examine the spatial distribution of I in the studied area. All wells selected as a part of this study exploit groundwater from the interface flowpath of the aquifer defined in Figure 2. Due to the control bedrock topography exhibits on the groundwater flow in the study area (Charron, 1975), bedrock elevation can be used as a proxy for distance from the recharge area (i.e. as bedrock elevation decreases, distance from the recharge area increases) as it travels along the interface flowpath. I concentrations in groundwater tend to increase as bedrock elevation decreases (Figure 4), implying that the highest I concentrations would be observed in depressions in the bedrock surface. Also shown in Figure 4 is the positive relationship between I concentrations and overburden (unconsolidated glacial sediment) thickness, which represents the combined thickness of the tills, subaqueous outwash deposits, glaciomarine muds, and nearshore sands. Where information on the representative geological unit sampled was available, this was compared to I concentrations (Figure 5). These units include carbonates (n = 99), shale (n = 13), glacial sediments (n = 23), and sandstone (n = 9). The highest median concentrations are observed in samples derived from shale units (1 327 µg/L) or glacial sediments (450 µg/L), whereas lower median concentrations are observed in samples derived from carbonate (129 µg/L) or sandstone (27 µg/L) units. I concentrations in samples taken from sandstone units appear to be significantly lower than from other units. High interquartile ranges are observable for samples from the carbonate, shale, and glacial sediment units.

311 *Principal component analysis*

312 The 19 chemical parameters for n = 146 sites retained for PCA (B, Ba, Br, Ca, Cl, DOC,
313 F, Fe, HCO_3, I, K, Li, Mg, Mn, Na, NH_4, Si, SO_4 and Sr) exhibited six factors accounting for
314 89% (41%, 16%, 10%, 8%, 7%, and 6% respectively) of the perceived variance in the dataset.
315 The results from PCA are presented in table 1, and the position of the loadings for each
316 parameter relative to principal components 1 and 2 are presented in Figure 6. Factor loadings >
317 ±0.7 were considered significant for the purposes of this analysis.

318 The first component is characterized by positive factor loadings for Na, K, HCO_3, Cl,
319 NH_4, Br, I, DOC, and B. The second component exhibits positive factor loadings for Ca and Mg,
320 in addition to a negative loading for F. Interpretations of the geochemical processes responsible
321 for significant factor loadings will be presented in the discussion. Each of remaining four
322 components do not exhibit significant loadings for I, explain less than 10% of variance within the
323 dataset and are more likely related to local effects than the first two components – thus, these
324 components were regarded as unimportant and not considered during the interpretation of PCA.
325 Component 3 exhibits a positive loading for Fe and Mn and most likely represents the reductive
326 dissolution of metal oxides, component 4 exhibits a positive loading for SO_4, component 5
327 exhibits a positive loading for Si, and component 6 a positive loading for Li.

328 *^{129}I*

329 Samples collected in 2016 analyzed for ^{129}I (n = 55) were separated into two groups
330 based on ^{3}H content, to qualitatively establish the presence of anthropogenic ^{129}I (Figure 7). As
331 per Clark and Fritz (1997), groundwaters lacking detectable proportions of ^{3}H (< 0.8 T.U.)
332 represent waters recharged prior to 1952, also referred to as “pre-modern” groundwaters.
333 Conversely, samples containing detectable proportions of ^{3}H (> 0.8 T.U.) represent either

recharge water dating after 1952 ("modern" groundwater) or a mix between pre-modern and modern groundwaters and would be affected by modern inputs of ^{129}I. Based on the classification from ^{3}H data, 21 samples analyzed for ^{129}I represent modern groundwater, whereas 34 represent pre-modern groundwaters. The data presented in in Figure 7 demonstrate a decrease of the $^{129}I/^{127}I$ ratio as I concentrations in a sample increase. Typically, modern waters exhibited $^{129}I/^{127}I$ ratios exceeding the pre-anthropogenic ratio of 150×10^{-14}, which can be attributed to the contribution of anthropogenic ^{129}I. The $^{129}I/^{127}I$ ratio for pre-modern groundwaters ranges from 5.7 to 460.7×10^{-14}, with an average of 62.4×10^{-14}. As I concentrations increase, the $^{129}I/^{127}I$ ratio decreases, and appears to remain constant around 20×10^{-14} after I concentrations surpass 500 µg/L. These trends represent a more important influence of geologic sources of I as concentrations increase.

DIC and DOC pools

The DIC pool in groundwater represents the sum of CO_2, HCO_3, and CO_3 species, the proportions of which vary based on pH. Given the range of pH values observed for collected samples (Figure 3), the DIC pool is expected to be predominantly comprised of the HCO_3 species. Potential sources for DIC in the groundwater aquifer include: (1) dissolved CO_2 soil gases from recharge waters, (2) CO_2 derived from the decomposition of dissolved or sedimentary organic carbon sources within overburden materials, (3) CO_2 derived from decomposition of dissolved or sedimentary organic matter within the Ordovician bedrock, and (4) HCO_3 derived from dissolution of carbonate bedrock. The relationship between ^{14}C ages for DIC and DOC with Cl and their respective $\delta^{13}C$ signatures is presented in Figure 8. Uncorrected ^{14}C ages for DIC were between 7.1 – 16.1 ka BP, with an average of 12.9 ka BP. $\delta^{13}C$ DIC values range from -23.3 to -5.1‰, and do not exhibit a significant relationship with uncorrected ^{14}C ages for DIC. A

lack of correlation also exists between uncorrected DOC ages with their respective $\delta^{13}C$ signatures. Uncorrected ^{14}C ages for DIC are youngest in low-salinity groundwaters, and stabilize at an age of approximately 15 ka BP at Cl concentrations exceeding 1000 mg/L. The same trend is observable for uncorrected DOC ages, although the "stable" age for samples with Cl concentrations > 1000 mg/L is approximately 16 ka BP. The similarity of the trends for the DIC and DOC pools suggest a relationship between the two.

Potential sources for DOC in the aquifer include: (1) soil organic carbon sources from recharge waters, (2) Organic matter generated during the Champlain Sea incursion, (3) Organic matter from the St. Pierre sediment, and (4) Organic matter from Ordovician bedrock. The first two components would present detectable proportions of radiocarbon, whereas the last two would not. ^{14}C ages for DOC from the current dataset vary from 4.4 – 19.3 ka BP, with an average of 13.5 ka BP. The average age corresponds to a time when the study area was still ice-covered, indicating a source of organic carbon which predates the Champlain Sea incursion. ^{14}C ages data for the disseminated organic matter within the glaciomarine mud presented in table 2 also suggests the presence of older organic carbon sources, as these ages range from 17.1 – 23.6 ka BP.

The $\delta^{13}C$ signature for disseminated organic carbon within the mud varies between -27.5 to -26.3‰, and averages -26.7‰. Additionally, the $\delta^{13}C$ signatures (n = 56, see electronic dataset) for DOC in groundwater vary from -29.72 to -25.86‰, with an average value of -26.8‰.

Discussion

Spatial distribution of I

The observed relationships for I with decreasing bedrock elevation and increasing overburden (glacial sediment) thickness are indicative of the enrichment of I in groundwater as it travels from recharge areas to depressions in the bedrock surface along the interface flowpath. A similar trend for groundwater salinization was observed by Montcoudiol et al. (2015) and Cloutier et al. (2006) for similar aquifers. They demonstrated that groundwater geochemical facies progressed from Ca-HCO_3 to Na-HCO_3 and finally Na-Cl with increasing distance from recharge areas. The main groundwater processes driving the transition from Ca-HCO_3 to Na-HCO_3 are ion exchange with the glaciomarine muds and carbonate dissolution as the solubility of carbonate increases due to Na^+ replacement by Ca^{2+} and Mg^{2+} in the mud matrix. The evolution of Na-HCO_3 to Na-Cl groundwater groups is mainly attributed to mixing with fossil Champlain Sea water (Cloutier et al., 2006). Box plots in Figure 9 show the dominant ion composition for groundwater samples relative to their I content and demonstrate that I enrichment is concurrent with system evolution and groundwater salinization, with values below 150 µg/L for Ca-HCO_3 waters (n =18), intermediate concentrations in Na-HCO_3 (n = 78) waters, and extreme concentrations over 1000 µg/L in Na-Cl (n = 46) waters. Samples in the Ca-SO_4/Cl portion of the Piper plot (n = 4) are characterized by their proximity to major roads, high Cl/Br ratios and detectable proportions of ^3H (> 0.8 T.U.), indicating that they likely represent modern groundwaters affected by road salt contamination.

Box-and-whisker plots for I concentrations relative to the geological setting of well screens indicate that higher concentrations are observed for groundwater sampled from shale and limestone units, whereas lower concentrations are observed for groundwater derived from

sandstone units. High I has been correlated to bedrock lithology in groundwaters sampled from shale (Lu et al., 2015; Hamilton et al., 2015) and limestone units (Fuge, 2005; Voutchkova et al., 2014), and attributed to the presence of marine organic matter in these rocks. However, evidence has also been presented in this paper suggesting that I is enriched with increasing distance from recharge areas. The spatial distribution of groundwater samples from sandstone units are predominantly found in the northern portion of the study area where bedrock elevations are higher and groundwater recharge is occurring, contrary to samples from limestone and shale units, which typically coincide with lower bedrock elevations where groundwater is of the Na-HCO_3 or Na-Cl geochemical facies, implying that I concentrations in groundwater may depend more on the spatial distribution of bedrock units rather than their lithology. High I concentrations for samples derived from glacial sediments also supports this interpretation, which agrees with results from Cloutier et al. (2006) for a similar interface aquifer in Québec, where they demonstrated that bedrock lithology does not control major ion chemistry, and instead attributed geochemical variations to hydrogeological conditions associated with surface sediments (unconfined, semi-confined, and confined aquifer conditions).

Principal Component Analysis (PCA)

Results from PCA indicate a significant relationship between I and major components of salinity (B, Br, Cl, and Na) as well as DOC, HCO_3, K, and NH_4 for the first component. Microbial decomposition of organic matter in the glaciomarine muds would release dissolved CO_2, causing a corresponding rise in HCO_3 concentrations. This is also reflected by the positive loading for DOC. The positive loading for K can also be explained due to the decomposition of organic matter, as suggested by average K concentrations for samples with > 1000 mg/L Cl^-, exceeding what would be expected with normal Cl/K ratios for seawater. The glaciomarine muds

have also been found by others to have high contents of exchangeable K (Laventure and Warkentin, 1965). Decomposition in an anaerobic environment would also result in the conversion of organic nitrogen to NH_4, and the conversion of organo-iodine to inorganic I, causing the enrichment of these elements in solution. Thus, factor loadings for component 1 are suggestive of saline porewaters within the glaciomarine muds enriched in I through the decomposition of marine organic matter. The high salinity of porewaters within the massive muds (Torrance, 1988), coupled with observations of hydrotroilite and evidence of bioturbation that are indicative bacterial reduction in the same massive muds (Cummings et al., 2011) suggests that I-rich saline porewater originates predominantly from the massive mud unit. Although the second component of the PCA does not exhibit significant loading for I, it explains an important proportion of the perceived variance (16%) within the dataset. Significant positive loadings for parameters relating to water hardness (Ca and Mg) and a negative loading for F were observed. These results are similar to findings from Cloutier et al. (2008) and Morton (2015) from geochemical characterizations of groundwater samples in similar aquifers, which were attributed to the decreased solubility of fluorite (CaF_2) due to increased proportions of dissolved Ca and Mg attributed to carbonate dissolution.

Significance for I and organic carbon sources in sediment loading of glacial meltwater

If the I in the glaciomarine muds were entirely derived from the marine basin, observed values for $^{129}I/^{127}I$ ratios would have reflected the pre-anthropogenic marine sediment ratio of 150×10^{-14}. However, the average observed ratio for pre-modern high-I groundwaters was much lower, at 20×10^{-14}. The depleted isotopic signature observed for ^{129}I would most likely be due to the introduction of allochthonous sources of ^{129}I-depleted geogenic I during the Champlain Sea incursion via glacial meltwater. Cloutier et al. (2006) demonstrated that glacial meltwater was a

448 significant component of the Champlain Sea. Analyses of modern-day glacial meltwaters
449 demonstrate that they can furnish the marine environment with important limiting micronutrients
450 such as Fe, DOC, NO_3, PO_4, and SiO_2, which would fertilize primary productivity (Hawkings et
451 al., 2015; Bhatia et al., 2013; Slemmons and Saros, 2012; Hodson et al., 2004). The authors are
452 not aware of any research conducted on I loading in glacial meltwaters.

453 PO_4 can serve as an analogue to interpret I export in glacial meltwater. Hodson et al.
454 (2004) remarked that PO_4 concentrations in glacial meltwater closely reflected the concentrations
455 of underlying sedimentary units. Similarly, in an analysis of the sources of ^{127}I and ^{129}I in coastal
456 watersheds of North America and Europe, Moran et al. (2002) demonstrated that rivers
457 surrounded by marine shale or carbonate sedimentary terrain show higher relative I
458 concentrations when compared to rivers surround by igneous or metamorphic bedrock. For rivers
459 unaffected by anthropogenic point sources of ^{129}I, they observed a depletion in the $^{129}I/^{127}I$ ratio
460 as I concentrations increased, which they attributed to the input of I derived from surrounding
461 bedrock or soils. This is in line with conclusions from Cohen (1985) postulating that I in fresh
462 surface waters is mainly derived from the weathering of sedimentary rocks. The stable $^{129}I/^{127}I$
463 ratio of approximately 20×10^{-14} observed for higher proportions of I exceeding 500 µg/L
464 suggests a significant proportion of I derived from carbonate and/or shale units. I is released into
465 solution both in its dissolved form as organic matter oxidation occurs, or as particulate organic
466 matter during physical weathering of the rock. Conversely, the $^{129}I/^{127}I$ values exceeding the pre-
467 anthropogenic ratio of 150×10^{-14} in pre-modern groundwaters can be attributed to the presence
468 of I derived from the weathering of sandstone or crystalline bedrock units.

469 As deglaciation proceeds, rock flour, typically of the clay and silt size fraction, is
470 evacuated from the subglacial environment by increasing meltwater flows. In the context of the

Champlain Sea, this rock flour would originate predominantly from weathering of local carbonate and shale bedrock units underlying the ice sheet. This would represent a significant input of particulate matter and limiting micronutrients into the Champlain Sea, resulting in an increase in primary production and subsequent I uptake as phytoplankton biomass increases. The ^{129}I and ^{127}I pools would reflect the mixing of allochthonous geogenic I sources exhibiting low $^{129}I/^{127}I$ ratios derived from surrounding sedimentary units with autochthonous sources having a pre-anthropogenic ratio of approximately 150×10^{-14}. Estimating mixing proportions from each source in this instance is difficult, due to the lack of data regarding glacial meltwater fluxes and their relative I concentrations in the Pleistocene.

Stable isotopic and ^{14}C evidence for the introduction of allochthonous sources of organic carbon through glacial meltwater was also presented for the organic carbon pools within the aquifer. The average uncorrected ^{14}C ages for both DOC (13.5 ka BP) and disseminated organic carbon (21.1 ka BP) correspond to a time when the study area was glaciated, and the large range of observed ^{14}C ages suggest mixing between sources with varying ages. Additionally, these ages exceed ones found for local freshwater shells in Bourget, Ontario (10.2 ± 0.1 ka BP; Gadd, 1980) and a marine algal bed in Ottawa (10.8 ± 0.2 ka BP; Mott, 1968).

While C:N atomic ratios below 10 for disseminated organic carbon within the glaciomarine muds suggest that the primary source of organic matter is marine phytoplankton (Meyers, 1994), the $\delta^{13}C$ signatures for this organic matter and DOC in groundwater are lower than what would be expected if organic carbon were derived solely from marine or estuarine phytoplankton, and overlap with the range for C_3 vegetation. This would suggest that mixing is occurring with an older C_3 vegetation source, which would most likely be introduced into the marine basin through glacial meltwater following abrasion of Paleozoic bedrock or proximal

494 interstadial deposits (e.g. St. Pierre sediment), both of which would present negligible ^{14}C
495 signatures. It is also interesting to note that the ^{14}C ages for disseminated organic matter
496 observed here are similar to results from Silliman et al. (1996) for a sediment core in Lake
497 Ontario, who also reported significantly older ^{14}C ages for disseminated organic matter relative
498 to ostracod shells, which they attributed to allochthonous sources of older detrital terrestrial
499 carbon in the disseminated organic pool introduced through streams and rivers.

500 Potential inorganic C sources within the aquifer were characterized using isotopic
501 analyses of radiocarbon and $\delta^{13}C$. When considering the mixing dynamics of DIC, soil gas (or
502 CO_2 generated from organic matter decomposition) is assumed to have a $\delta^{13}C$ signature of -25‰
503 with a radiocarbon content corresponding to the age of the organic matter, while carbonate is
504 assumed to have a $\delta^{13}C$ signature of 0‰, with a negligible radiocarbon content (Pearson and
505 Hanshaw, 1970). Groundwaters in closed systems where the two sources of DIC are at
506 equilibrium commonly present $\delta^{13}C$ values around -12‰ for DIC.

507 The average uncorrected ^{14}C ages for DIC (12.9 ka BP) roughly correspond to the
508 Champlain Sea incursion. However, the study area was ice-covered until approximately 12 ka
509 BP before glacial retreat (Parent and Ochietti, 1988), which would imply that ages exceeding 12
510 ka BP represent samples where older carbon sources have been added to the DIC pool. As
511 observed in Figure 10, depleted $\delta^{13}C$ signatures of DIC (< -12‰) as HCO_3 concentrations
512 increase suggests that the DIC pool is predominantly influenced by decomposition of organics
513 (most likely in the massive muds) rather than carbonate dissolution. Additionally, the proximity
514 of the uncorrected DIC radiocarbon ages to the timing of the Champlain Sea incursion indicate
515 that DIC derived from the decomposition of contemporaneous autochthonous marine organic
516 matter is the primary carbon source in the DIC pool.

Following the retreat of the Champlain Sea ~10 ka BP (Parent and Ochietti, 1988) was a period of high flow for the Ottawa River as it re-established its main channel, lasting from 10 - 4.7 ka BP (Fulton, 1987). Evidence for these high flows is present in the study area in the form of anastomosed river channels incised in the glaciomarine sediments (Russell et al., 2011). During this period of high flow, infiltration of freshwater into the interface aquifer and mixing with remnant Champlain Sea water would have occurred. No samples analyzed for radiocarbon contained any detectable ^{3}H (< 0.8 T.U.), which would preclude sources of modern freshwater carbon. Thus, the infiltration of freshwater from the paleo Ottawa River could potentially explain the prevalence of uncorrected radiocarbon ages < 10 ka BP in both the DIC and DOC at low proportions of Cl, as the infiltrating freshwater would contain younger (but still sub-modern) sources of organic and inorganic carbon.

Conclusions

The spatial patterns, enrichment mechanisms, and sources of I and organic matter in Eastern Ontario groundwater were characterized using a regional geochemical dataset that included ^{129}I and ^{14}C radiogenic tracers. Concentrations of I exceeding 150 µg/L were prevalent in Na-Cl geochemical facies, and most often observed in depressions in the bedrock surface overlain by thick layers of glacial sediments. Although the influence of bedrock lithology on I concentrations cannot be ignored, it is likely not a dominant factor. Geochemical and multivariate statistical analysis confirm the hypothesis that high I in groundwaters is due to the intrusion of saline porewaters from the massive muds enriched in I through microbial oxidation of organic matter, particularly marine algae, which was shown to be the primary source of organic matter in the mud matrix. Groundwater residence times estimated by ^{14}C analysis demonstrate that saline groundwater within the study area represents remnant lenses of

Champlain Sea water. ^{129}I analysis of I in groundwaters suggests mixing between autochthonous marine and allochthonous geogenic I sources in the Champlain Sea basin, derived from the weathering of surrounding Paleozoic sedimentary rocks, and transported into the Champlain Sea with glacial meltwaters. Glacial meltwaters would also introduce older, allochthonous sources of organic carbon derived from the mechanical erosion of Paleozoic bedrock and local interstadial organic units, as evidenced by ^{14}C ages for DOC in groundwaters and disseminated organic carbon within the mud. $\delta^{13}C$ values indicate that the allochthonous organic matter in mud is likely C_3 vegetation. Future work should aim to better characterize drainage patterns and pre-Champlain Sea organic carbon pools in the Eastern Ontario region in an effort to constrain the source of allochthonous organic matter in the Champlain Sea basin. In the context of public health issues, this study represents a significant first step in the delineation of areas where high I concentrations in groundwater may pose a significant health risk for consumers. This would be applicable not only to the studied area, but also to geologically similar aquifers in Eastern Canada affected by the Champlain Sea incursion.

Acknowledgements

The authors would like to acknowledge field assistance provided by J. Dyer, N. McClenaghan, and C. Rogerson, assistance in preparation of stable and radiogenic isotope samples from K. Klassen, P.Wickham, S. Murseli, and M. Wilk, and the hospitality of all homeowners who participated in the study.

References

Andersen, S., Petersen, S.B., Laurberg, P., 2002. Iodine in drinking water in Denmark is bound in humic substances. *European Journal of Endocrinology* 147: 663–670.

Andersen, S., Guan,H.X., Teng,W.P., Laurberg, P., 2008. Speciation of iodine in high iodine groundwater in China associated with goiter and hypothyroidism. Biological Trace Element Research 128, 95–103

Armstrong, D.K. and Dodge, J.E.P. 2007. Paleozoic geology of southern Ontario. *Ontario Geological Survey*, **Miscellaneous Release—Data 219** – Revised.

Barnett, P.J. 1992. Quaternary Geology of Ontario. **Geology of Ontario;** *OGS Special Volume 4, Chapter 21.* Ministry of Northern Development and Mines, 2nd edition.

Bhatia, M.P., Kujawinski, E.B., Das, S.B., Breier, C.F., Henderson, P.B., and Charette, M.A. (2013) Greenland meltwater as a significant and potentially bioavailable source of iron to the ocean. *Nature Geoscience* 6, 274-278.

Castro, S.I.B, R. Berthiaume, P. Laffey, A. Fouquet, F. Beraldin, A. Robichaud and P. Lacasse. 2010. Iodine concentration in milk sampled from Canadian farms. *Journal of Food Protection,* 73(9):1658-1663.

Chapuis, R., and Saucier, A. 2013. A Leaky Aquifer below Champlain Sea Clay: Closed-Form Solutions for Natural Seepage. *Groundwater*, 51(6):960-967.

Charron, J.E. (1975). A study of groundwater flow in Russell County, Ontario. Environment Canada, Inland Waters Dir. Sci. Ser. No. 40, 26 pp.

Chen, J., Liu, D., Peng, P., Ning, C., Xiaolin, H., Zhang, B., and Zhongyao, X. (2016). Iodine-129 chronological study of brines from an Ordovician paleokarst reservoir in the Lunnan oilfield, Tarim Basin. *Applied Geochemistry,* 65: 14-21.

China Ministry of Health 2003. Classification of areas with high iodine in water and endemic areas of goiter; China National Standard GB/T 19380-2003, p.1-2 [in Chinese with English abstract].

Clark, I., and Fritz, P. (1997). Environmental Isotopes in Hydrogeology. Boca Raton, FL, CRC Press.

Cloutier, V., Lefebvre, R., Savard, M., Bourque, E., and Therrien, R. 2006. Hydrogeochemistry and groundwater origin of the Basses-Laurentides sedimentary rock aquifer system, St. Lawrence Lowlands, Québec, Canada. *Hydrogeology Journal*, 14(4): 573-590.

Cloutier, V., Lefebvre, R., Therrien, R., and Savard, M. (2008). Multivariate statistical analysis of geochemical data as indicative of the hydrogeochemical evolution of groundwater in a sedimentary rock aquifer system. *Journal of Hydrology*, 353(3-4): 294-313.

Cloutier, V., Lefebvre, R., Savard, M.M., and Therrien, R. (2010). Desalination of a sedimentary rock aquifer system invaded by Pleistocene Champlain Sea water and processes controlling groundwater geochemistry. *Environmental and Earth Sciences,* 59 (5), 977–994.

Cohen, B. L. (1985). The origin of I in soil and the 129I problem, *Health Physical*, 49(2), 279–285.

Crann, C.A., Murseli, S., St□Jean, G., Zhao, X., Clark, I.D., and Kieser, W.E. 2017. First status report on radiocarbon sample preparation at the A.E. Lalonde AMS Laboratory (Ottawa, Canada). *Radiocarbon* 59(3): 695–704.

Cummings, D. I., Gorrell, G., Guilbault, J. P., Hunter, J. A., Logan, C., Ponomarenko, D., and Sharpe, D. R. (2011). Sequence stratigraphy of a glaciated basin fill, with a focus on esker sedimentation. *Bulletin of the Geological Society of America*, *123*(7–8), 1478–1496.

Di Iorio, T., Lemieux, A.J. and Hamilton, S.M. 2015. Township of Alfred and Plantagenet groundwater study; in Summary of Field Work and Other Activities 2015, Ontario Geological Survey, Open File Report 6313, p.38-1 to 38-6.

Donovan, J., and Lajoie, G. (1979). Geotechnical implications of diagenetic iron sulphide formation in Champlain Sea sediments. *Canadian Journal of Earth Sciences*, 16: 575-584.

Duan, L., Wang, W., Sun, Y., and Zhang, C. (2016). Iodine in groundwater of the Guanzhong Basin, China: sources and hydrogeochemical controls on its distribution. *Environmental Earth Sciences*, 75:790.

Fabryka-Martin, J., H. Bentley, D. Elmore, and P. Airey (1985), Natural iodine-129 as an environmental tracer, Geochim. Cosmochim. Acta, 49(2), 337–347, doi:10.1016/0016-7037(85)90027-4.

Fabryka-Martin, J., Whittemore, D. O., Davis, S. N., Kubik, P. W., & Sharma, P. (1991). Geochemistry of halogens in the Milk River aquifer, Alberta, Canada. *Applied Geochemistry*, *6*(4), 447–464.

Fehn., U. (2000). Dating of pore waters with 129I: Relevance for the origin of marine gas hydrates. *Science*, 289(5488): 2332-2335.

Freckelton, C.N. and Hamilton, S.M. 2012. Ambient Groundwater Geochemistry Project of the Ottawa–St. Lawrence River area; in Summary of Field Work and Other Activities 2012, Ontario Geological Survey, Open File Report 6280, p.37-1 to 37-7.

Fuge, R., Johnson, C.C., 1986. The geochemistry of iodine—a review. Environmental Geochemistry and Health 8 (2), 31–54.

Fuge, R. (2005). Soils and Iodine Deficiency. In O. Selinus, B. J. Alloway, J. A. Centeno, R. B. Finkelman, R. Fuge, U. Lindh, et al. (Eds.), *Essentials of medical geology: Impacts of the natural environment on public health* (pp. 417–433). Amsterdam: Elsevier.

Fulton, R. 1987. Quaternary Geology of the Ottawa Region, Ontario and Quebec. *Geological Survey of Canada,* **Paper 86-23.**

Gadd, N.R. (1980). Maximum age for a concretion at Green Creek, Ontario. *Géographie physique et Quaternaire*, 34(2) : 229-238.

Gadd, N.R. (1986). Lithofacies of Leda clay in the Ottawa basin of the Champlain Sea: Geological Survey of Canada Paper 85-21, 44 p. ISBN 0-660-12089-5.

Gao, C., Shirota, J., Kelly, R. I., Brunton, F.R. and van Haaften, S. 2006. Bedrock topography and overburden thickness mapping, southern Ontario; Ontario Geological Survey, Miscellaneous Release—Data 207.

Goldschmidt, V.M. 1954. Geochemistry. Oxford University Press, London.

Güler, C., Thyne, G., McCray, J., Turner, K. (2002). Evaluation of graphical and multivariate statistical methods for classification of water chemistry data. *Hydrogeology Journal,* 10(4):455–474.

Hamilton, S. M., Grasby, S. E., McIntosh, J. C., & Osborn, S. G. (2015). The effect of long-term regional pumping on hydrochemistry and dissolved gas content in an undeveloped shale-gas-bearing aquifer in southwestern Ontario, Canada. *Hydrogeology Journal*, *23*(4), 719–739.

Hawkings, J., Wadham, J., Tranter, M., Lawson, E., Sole, A., Cowton, T., Tedstone, A.J., Bartholomew, I., Nienow, P., Chandler, D., and Telling, J. (2015). The effect of warming climate on nutrient and solute export from the Greenland Ice Sheet. *Geochemical Perspectives Letters*, I: 94-104.

Health Canada (2017). Guidelines for Canadian Drinking Water Quality—Summary Table. Water and Air Quality Bureau, Healthy Environments and Consumer Safety Branch, Health Canada, Ottawa, Ontario.

Herod, M. 2015. Tracing the transport, geochemical cycling and fate of Iodine-129 in earth surface reservoirs. Ph.D. thesis, Department of Earth and Environmental Sciences, University of Ottawa, Ottawa, ON.

Hodson, A.J., Mumford, P., and Lister, D. (2004) Suspended sediment and phosphorus in proglacial rivers: bioavailability and potential impacts upon the P status of ice-marginal receiving waters. *Hydrological Processes* 18, 2409-2422.

Kashiwagi, H., Shikazono, N., Ogawa, Y., Higuchi, Y., Takahashi, M., & Tanaka, Y. (2006). Mineralogical and biological influences on groundwater chemistry of the Boso Peninsula, Chiba, central Japan: Implications for the origin of groundwater in sedimentary basins. *Geochemical Journal*, *40*(4), 345–361.

Laventure, B, and Warkentin, R.S. (1965). Chemical properties of Champlain Sea sediments. *Canadian Geotechnical Journal*, 2: 299-308

675 Lemieux, A.J., Clark, I.D., Hamilton, S.M., Rogerson C.M. and Kelton, D.F., 2016. The
676 provenance of, and possible relationship between, methane and halogens in groundwater
677 in southeastern Ontario. Ontario Geological Survey Summary of Field Work and Other
678 Activities, 2016, p. 33.1 to 33.7.

679 Li, J., Wang, Y., Xie, X., and Gao, W. (2013). Hydrogeochemistry of high iodine groundwater: a
680 case study at the Datong Basin, northern China. *Environmental Science Processes &*
681 *Impacts*. 15(4): 848-859.

682 Lu, Z., Hummel, S. T., Lautz, L. K., Hoke, G. D., Zhou, X., Leone, J., & Siegel, D. I. (2015).
683 Iodine as a sensitive tracer for detecting influence of organic-rich shale in shallow
684 groundwater. *Applied Geochemistry*, *60*, 29–36.

685 Malcolm, S. J., & Price, N. B. (1984). The behaviour of iodine and bromine in estuarine surface
686 sediments. *Marine Chemistry*, *15*(3), 263–271.

687 Meyers, P.A. (1994). Preservation of elemental and isotopic source identification of sedimentary
688 organic matter. *Chemical Geology*, 114: 289-302.

689 Moisan TA, Dunstan WM, Udomkit A, Wong GTF. (1994). The uptake of iodate by marine
690 phytoplankton. *Journal of Phycology,* 30:580–587.

691 Montcoudiol, N., Molson, J., Lemieux, J. M., & Cloutier, V. (2015). A conceptual model for
692 groundwater flow and geochemical evolution in the southern Outaouais Region, Québec,
693 Canada. *Applied Geochemistry*, *58*, 62–77.

694 Mott, R.J. (1968). A radiocarbon-dated marine algal bed of the Champlain Sea episode near
695 Ottawa, Ontario. *Canadian Journal of Earth Sciences*, 5: 319-323.

696 Moran, J., Oktay, S., and Santschi, R. (2002). Sources of iodine and iodine 129 in rivers. *Water*
697 *Resources Research*, 38(8): 24-1 to 24-10.

698 Morton, S.R., Di Iorio, T., Hamilton, S.M. and Robin, M.J.L. 2013. Development of an aquifer
699 mapping tool, City of Clarence–Rockland, Ontario; in Summary of Field Work and Other
700 Activities 2013, Ontario Geological Survey, Open File Report 6290, p.40-1 to 40-7.

701 Morton, S. (2015). Development and Evaluation of an Aquifer Capability Screening Tool
702 (ACST) – Pilot Study: Clarence-Rockland, Ontario. M.Sc. Thesis, University of Ottawa,
703 Ottawa, Ontario, Canada.

704 Ochietti, S. 1989. Quaternary geology of St. Lawrence Valley and adjacent Appalachian
705 subregion. In: Fulton, R.J. (Ed.), Quaternary Geology of Canada and Greenland. Geology
706 of Canada Series, No 1, pp. 350-389. ISBN 0-660-13114-5.

707 Ontario Geological Survey (OGS). 2010. Surficial geology of southern Ontario; Ontario
708 Geological Survey, Miscellaneous Release— Data 128 – Revised.

709 Ontario Geological Survey (OGS). Ambient Groundwater Geochemistry Data in GIS format.
710 Consulted September 26, 2016. Retrieved from http://www.mndm.gov.on.ca/en/mines-
711 and-minerals/applications/ogsearth/ambient-groundwater-geochemistry

712 Parent M, Occhietti S (1988) Late Wisconsinian deglaciation and Champlain Sea invasion in the
713 St. Lawrence Valley, Québec. *Géographie physique et Quaternaire,* 42: 215–246.

714 Pearson, F.J., Hanshaw Jr., B.B., 1970. Sources of dissolved carbonate species in groundwater
715 and their effects on carbon-14 dating. Isotope Hydrology 1970. IAEA, Vienna, pp. 271–
716 286.

717 R Core Team (2016). R: A language and environment for statistical computing. R Foundation for
718 Statistical Computing, Vienna, Austria. URL https://www.R-project.org/.

719 Rädlinger,G., Heumann, K. G. (2000). Transformation of iodide in natural and wastewater
720 systems by fixation on humic substances. *Environ. Sci. Technol*. 34(18), 3932.

721 Rao, U., and Fehn, U. (1999). Sources and reservoirs of anthropogenic Iodine-129 in western
722 New York. *Geochimica et Cosmochimica Acta*, 63: 1927-1938.

723 Rogerson C.M., Kelton, D.F., Hamilton, S.M., Lemieux, A.J., and Clark, I.D. 2016. The
724 investigation of groundwater as a source of high iodine levels in milk from dairy herds in
725 Eastern Ontario. Ontario Geological Survey Summary of Field Work and Other
726 Activities, 2016, p. 34.1 to 34.5.

727 Russell, H.A.J., Brooks, G.R., and Cummings, D.I. (ed.), 2011. Deglacial history of the
728 Champlain Sea basin and implications for urbanization; Joint annual meeting GAC-
729 MAC-SEG-SGA, Ottawa, Ontario, May 25–27, 2011; Fieldtrip guidebook; Geological
730 Survey of Canada, Open File 6947, 96 p. doi:10.4095/289555

731 Sanford, R.F., Pierson, C.T., and Crovelli, R.A. (1993). An objective replacement method for
732 censored geochemical data. *Math Geol* 25: 59–80.

733 Silliman, J., Meyers, P., and Bourbonniere, R. (1996). Record of postglacial organic matter
734 delivery and burial in sediments of Lake Ontario. *Organic Geochemistry*, **24**(4): 463-472.

735 Slemmons K.E.H., and Saros J.E. (2012). Implications of nitrogen-rich glacial meltwater for
736 phytoplankton diversity and productivity in alpine lakes. *Limnology and Oceanography*
737 57:1651–1663.

738 Stats Canada. 2016. “Community profile – 2011 census”.

739 Stats Canada. 2013. “Iodine status of Canadians, 2009 to 2011”.

740 Thompson, M., and Howarth, R.J. (1978). A new approach to the estimation of analytical
741 precision. *Journal of Geochemical Exploration* 9: 23-30.

742 Togo, Y. S., Takahashi, Y., Amano, Y., Matsuzaki, H., Suzuki, Y., Terada, Y., Iwatsuki, T.
743 (2016). Age and speciation of iodine in groundwater and mudstones of the Horonobe area,
744 Hokkaido, Japan: Implications for the origin and migration of iodine during basin evolution.
745 *Geochimica et Cosmochimica Acta*, *191*, 165–186.

746

Torrance, J.K., 1988, Mineralogy, pore-water chemistry, and geotechnical behaviour of Champlain Sea and related sediments, p. 259–275, *in* Gadd, N.R., ed., The Late Quaternary Development of the Champlain Sea Basin: Geological Association of Canada Special Paper 35, 312 p. ISBN 0-919216-35-8.

Veillette, J. J. and Nixon, F. M., 1984. Sequence of Quaternary sediments in the Bélanger sand pit. Pointe-Fortune. Québec-Ontario. Géographie physique et Quaternaire. 38: 59-68.

Voutchkova, D. D., Kristiansen, S. M., Hansen, B., Ernstsen, V., Sørensen, B. L., & Esbensen, K. H. (2014). Iodine concentrations in Danish groundwater: historical data assessment 1933–2011. *Environmental Geochemistry and Health*, *36*(6), 1151–1164.

Voutchkova, D., Ernsten, V., Kristiansen, S., and Hansen, B. (2017). Iodine in major Danish aquifers. *Environmental Earth Sciences,*

WHO. (2007). Iodine deficiency in Europe: A continuing public health problem. In M. Andersson, B. de Benoist, I. Darnton-Hill, & F. Delange (Eds.), (pp. 1–86). France: World Health Organization, UNICEF.

Zhang, E.Y., Zhang, F.C., Qian, Y., Ye, N.J., Gong, J.S., Wang, Y.S. (2010). The distribution of high iodine groundwater in typical areas of China and its inspiration. *Geology in China* 37 (3), 797–802 (in Chinese with English abstract).

Zhang, E., Wang, Y., Qian, Y., Ma, T., Zhang, D., Zhan, H., and Wang, S. (2013). Iodine in groundwater of the North China Plain: Spatial patterns and hydrogeochemical processes of enrichment. *Journal of Geochemical Exploration*, *135*, 40–53.

Tables

Table 1. PCA Eigenvalues, explained variance percentages, and Varimax-normalized factor loadings. Significant factor loadings (> ±0.7) are shown with bold text.

Parameter	Component 1	Component 2	Component 3	Component 4	Component 5	Component 6
Ca	-0.17	**0.81**	0.33	0.36	0.11	0.09
Mg	0.50	**0.72**	0.31	0.20	0.11	0.01
Na	**0.92**	0.01	-0.01	-0.01	-0.15	0.17
K	**0.87**	0.25	0.25	-0.12	0.05	0.07
HCO_3	**0.89**	0.01	-0.01	-0.10	0.15	-0.10
SO_4	-0.51	0.09	0.00	**0.80**	0.05	-0.04
NH_4	**0.83**	-0.11	0.26	-0.25	0.09	0.11
F	0.02	**-0.92**	-0.12	0.08	0.03	-0.07
Iodide	**0.94**	0.03	0.09	-0.09	-0.01	0.12
DOC	**0.70**	-0.37	-0.03	-0.14	0.13	-0.43
B	**0.84**	-0.39	0.00	-0.09	-0.01	0.25
Sr	0.30	0.46	0.25	0.62	0.21	0.21
Si	-0.16	0.02	0.08	0.13	**0.93**	-0.03
Ba	0.53	0.40	0.02	-0.41	0.51	0.05
Cl	**0.82**	0.35	0.03	0.10	-0.21	0.17
Br	**0.89**	0.19	0.05	0.02	-0.17	0.24
Li	0.43	0.12	0.04	0.03	-0.01	**0.84**
Fe	0.30	0.13	**0.86**	0.05	0.17	-0.08
Mn	-0.07	0.38	**0.84**	0.05	-0.08	0.14
Explained variance	7.87	3.09	1.89	1.53	1.37	1.2
Explained variance (%)	41	16	10	8	7	6
Cumulative % of variance	41	58	68	76	83	89

795 **Table 2**. Dataset for disseminated organic matter within glaciomarine muds. GC represents
796 samples collected from Green's Creek, whereas EME/EMW represents samples collected in
797 Embrun. pMC = % modern carbon
798

Sample ID	Radiocarbon laboratory no.	C:N	$\delta^{13}C$	pMC	^{14}C age	Error
		atomic ratio	‰ VPDB	%	^{14}C ka BP	± years
GC-2	UOC-5233	8.8	-26.3	5.31	23.6	209
GC-3	UOC-5234	8.1	-26.5	5.76	22.9	136
GC-4	UOC-5235	8.9	-26.4	6.66	21.7	151
EME	UOC-5237	9.4	-27.5	11.94	17.1	76
EMW	UOC-5236	9.2	-27.2	7.83	20.5	115

799
800
801
802
803
804
805
806
807
808
809
810
811
812

Figure Captions

Figure 1. Location of groundwater samples and I concentrations relative to (a) bedrock topography, (b) surficial geology, and (c) bedrock lithology. Star represents Green's Creek site where mud samples were collected, whereas X represents Embrun sample site. Universal Transverse Mercator (UTM) co-ordinates provided using North American Datum 1983 (NAD83) in Zone 18N. *Map data acquired from OGS MRD 219 (Armstrong & Dodge, 2007), 207 (Gao et al., 2006) & 128 (OGS, 2010.*

Figure 2. Conceptual model of the flow regime in the studied regional aquifer. *Modified from Cloutier et al. (2010).*

Figure 3. Pourbaix diagram with Eh-pH values for collected groundwater samples.

Figure 4. I concentrations relative to bedrock elevation and overburden thickness.

Figure 5. Box-and-whisker plots of I relative to geological setting of well screen.

Figure 6. Plot of loadings for the first two components of the Varimax normalized rotation.

Figure 7. $^{129}I/^{127}I$ ratio vs. I concentrations. Pre-anthropogenic $^{129}I/^{127}I$ seawater ratio of 150×10^{-14} indicated by the dashed line. Effect of influences from anthropogenic or geological sources of I indicated by arrows. Open circles represent modern groundwaters, whereas closed circles represent post-modern groundwaters.

Figure 8. Uncorrected ^{14}C ages of DIC and DOC plotted against Cl content and their respective $\delta^{13}C$ signatures. Closed circles represent DIC samples, whereas open circles represent DOC samples.

Figure 9. (a) Piper plot representing that major ion chemistry of groundwater samples. Numbers 1, 2, 3, and 4 represent the Ca-HCO_3, Na-HCO_3, Na-Cl, and Ca-SO_4/Cl groundwater geochemical facies, respectively. (b) Box-and-whisker plots of I concentration relative to geochemical facies of groundwater samples.

Figure 10. $\delta^{13}C$ DIC vs HCO_3 concentrations.

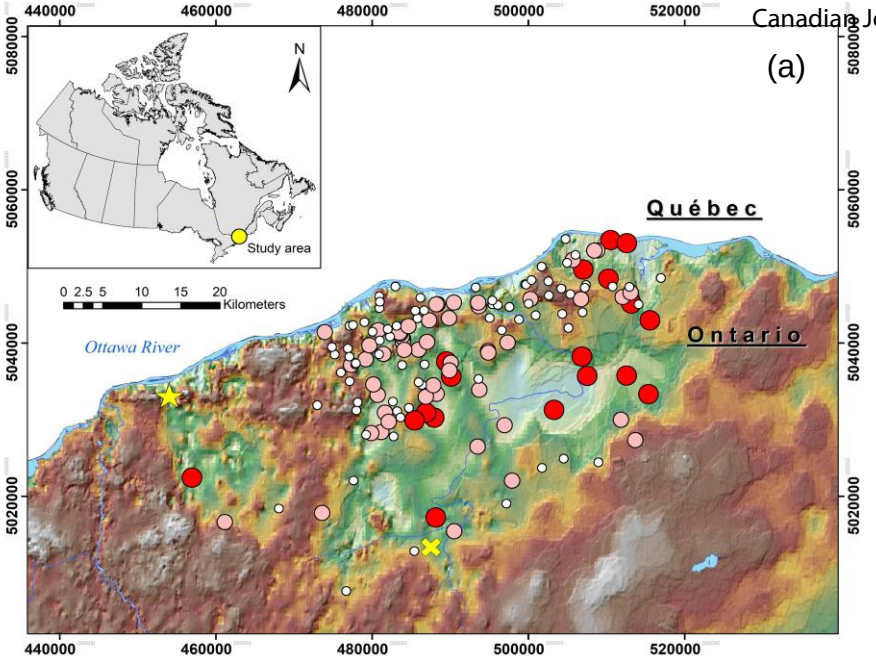

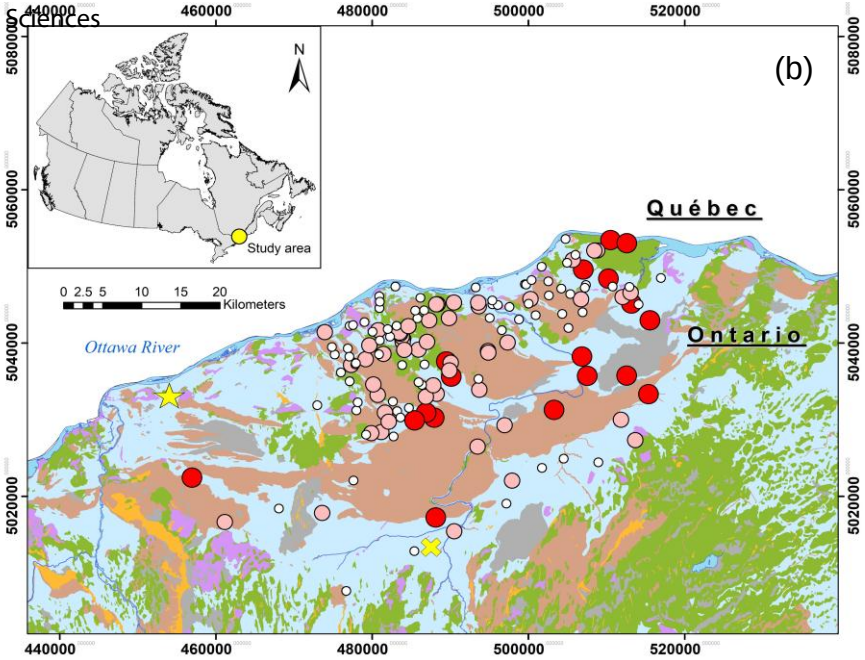

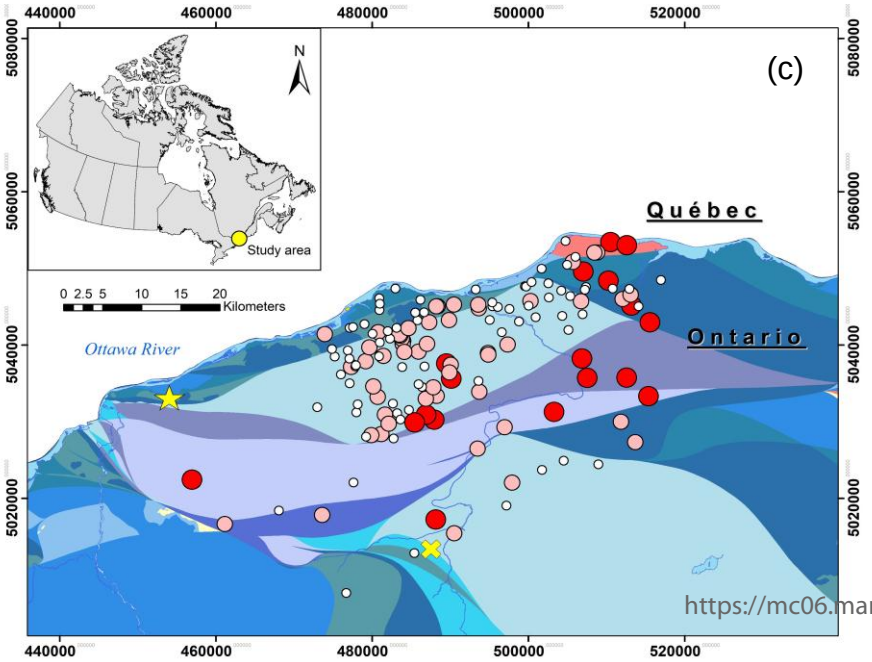

Legend

I (ug/L)

- < 150
- 150 - 1000
- > 1000

Bedrock elevation (mASL)

- High : 129
- Low : -50

Surficial geology

- Paleozoic Bedrock
- Precambrian Bedrock
- clay
- diamicton
- gravel
- organic deposits
- sand

Bedrock Unit

- 16: Queenston
- 15: Carlsbad
- 13: Billings
- 11: Lindsay
- 10: Verulam
- 9: Bobcaygeon
- 8: Gull River
- 6: Rockcliffe
- 5: Oxford
- 4: March
- 3: Nepean
- 2: Covey Hill
- 1: Precambrian

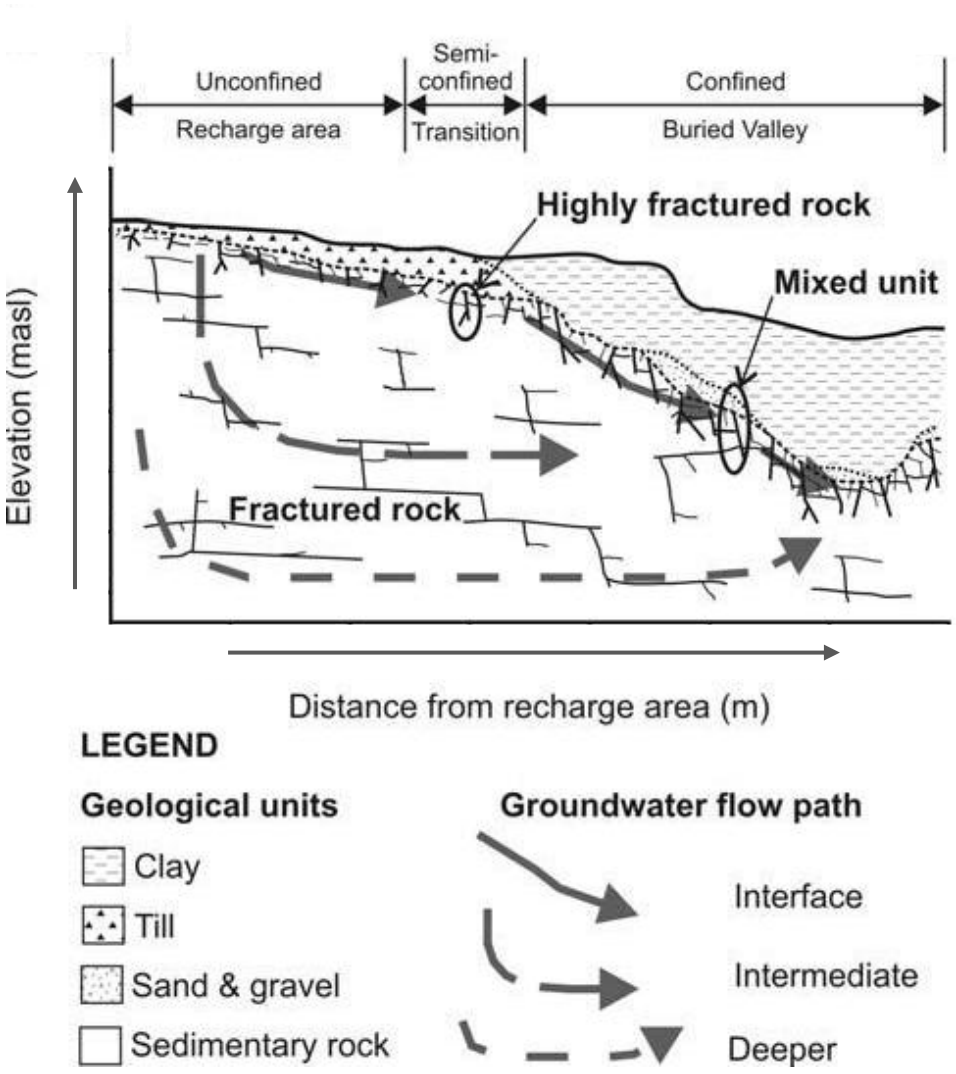
Unconfined
Recharge area
Semi-confined
Transition
Confined
Buried Valley
Highly fractured rock
Mixed unit
Fractured rock
Elevation (masl)
Distance from recharge area (m)
LEGEND
Geological units
Clay
Till
Sand & gravel
Sedimentary rock
Groundwater flow path
Interface
Intermediate
Deeper

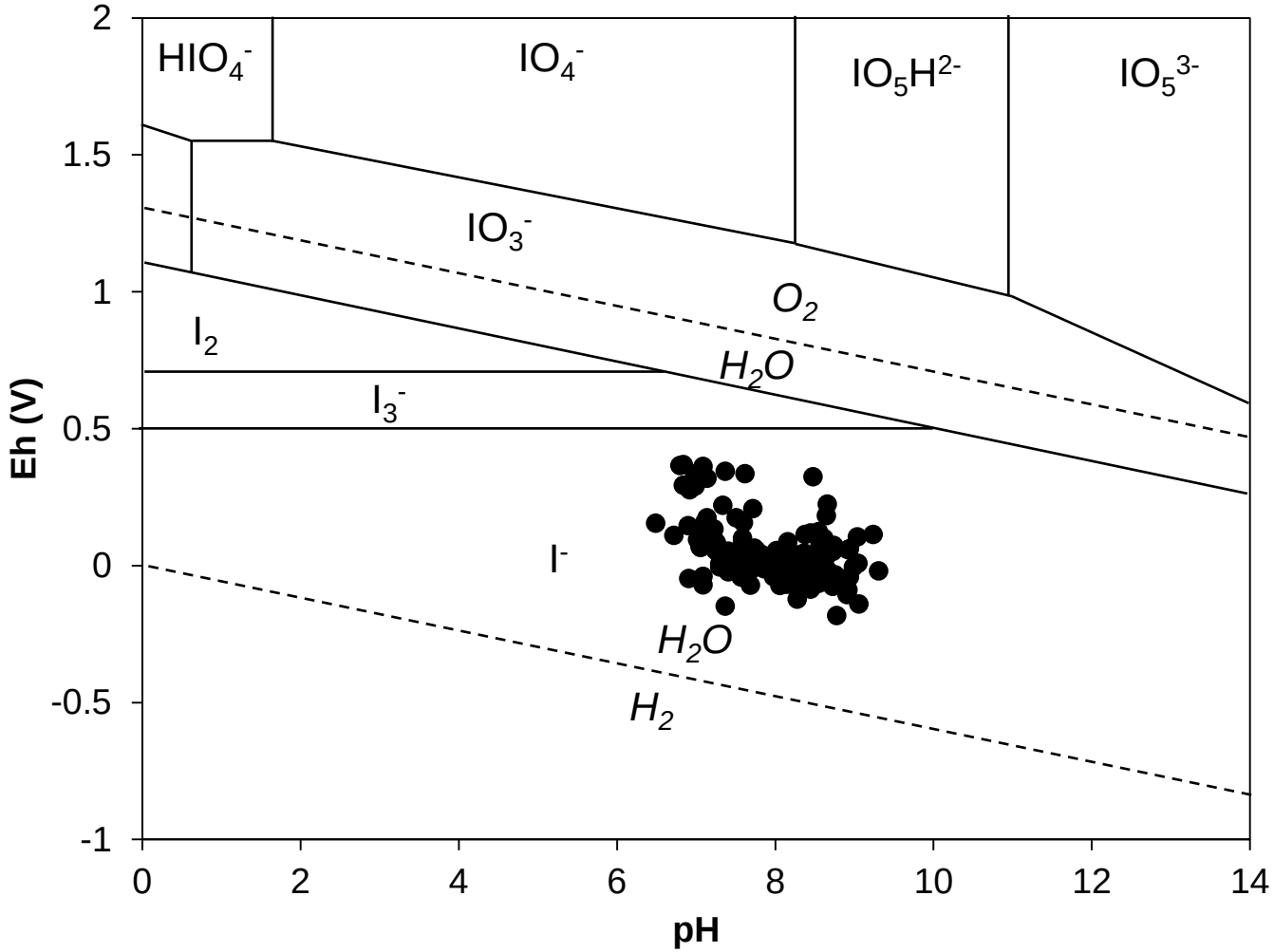
HIO4-
IO4-
IO5H2-
IO5 3-
IO3-
O2
I2
H2O
I3-
I-
H2O
H2
Eh (V)
pH
2
1.5
1
0.5
0
-0.5
-1
0
2
4
6
8
10
12
14

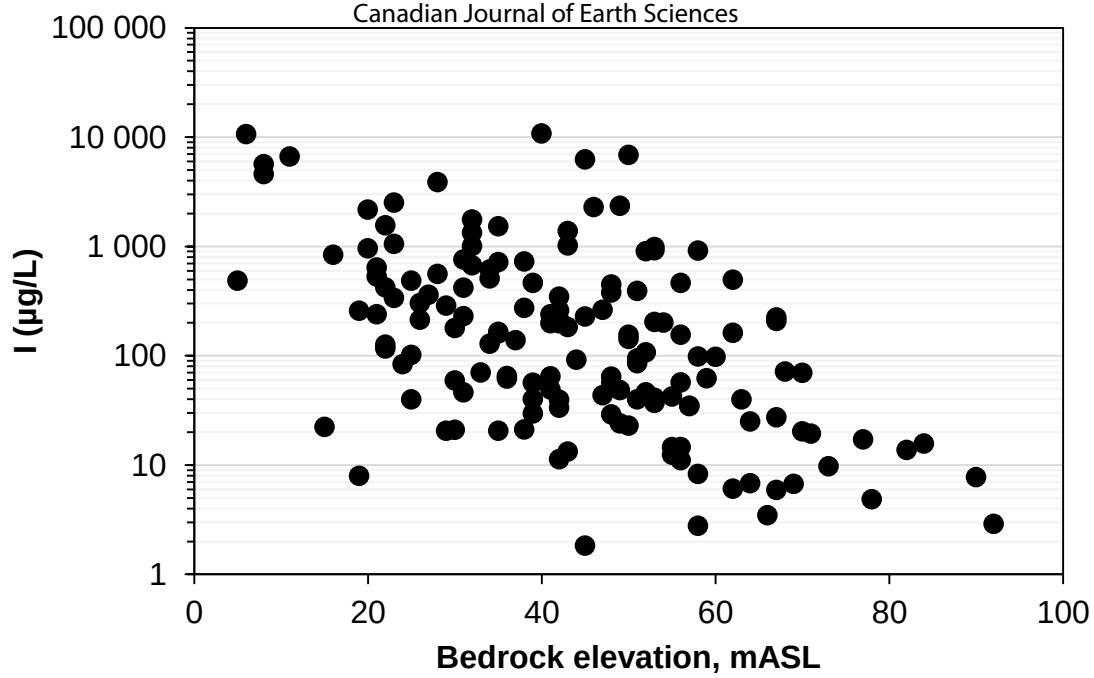
100 000
10 000
1 000
100
10
1
I (µg/L)
0
20
40
60
80
100
Bedrock elevation, mASL

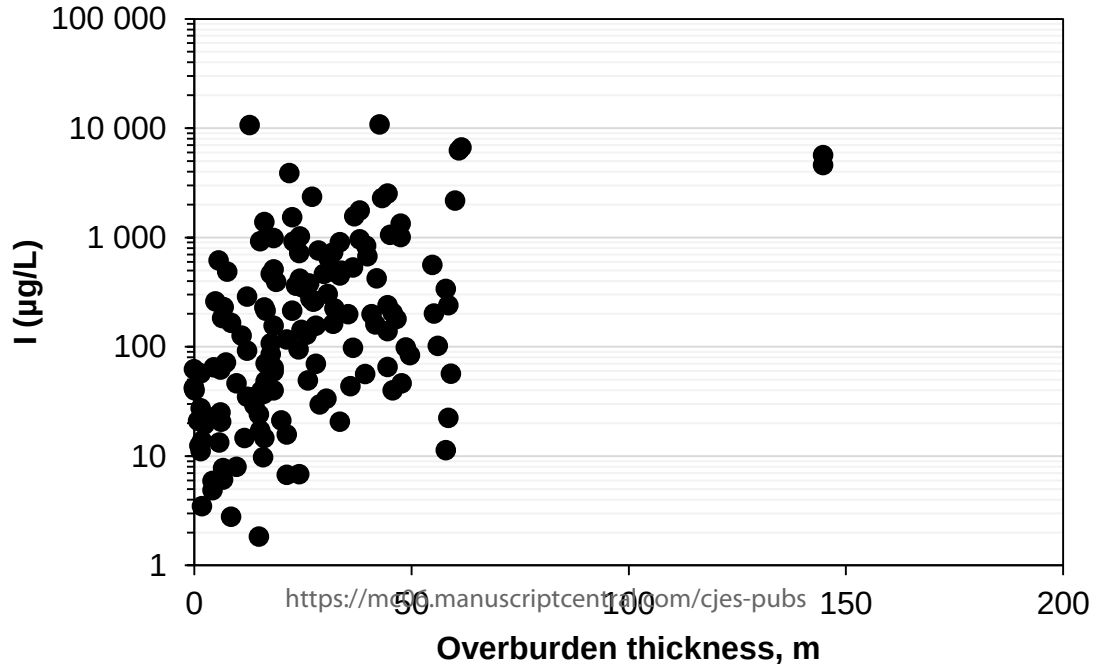
100 000
10 000
1 000
100
10
1
I (µg/L)
0
50
100
150
200
Overburden thickness, m

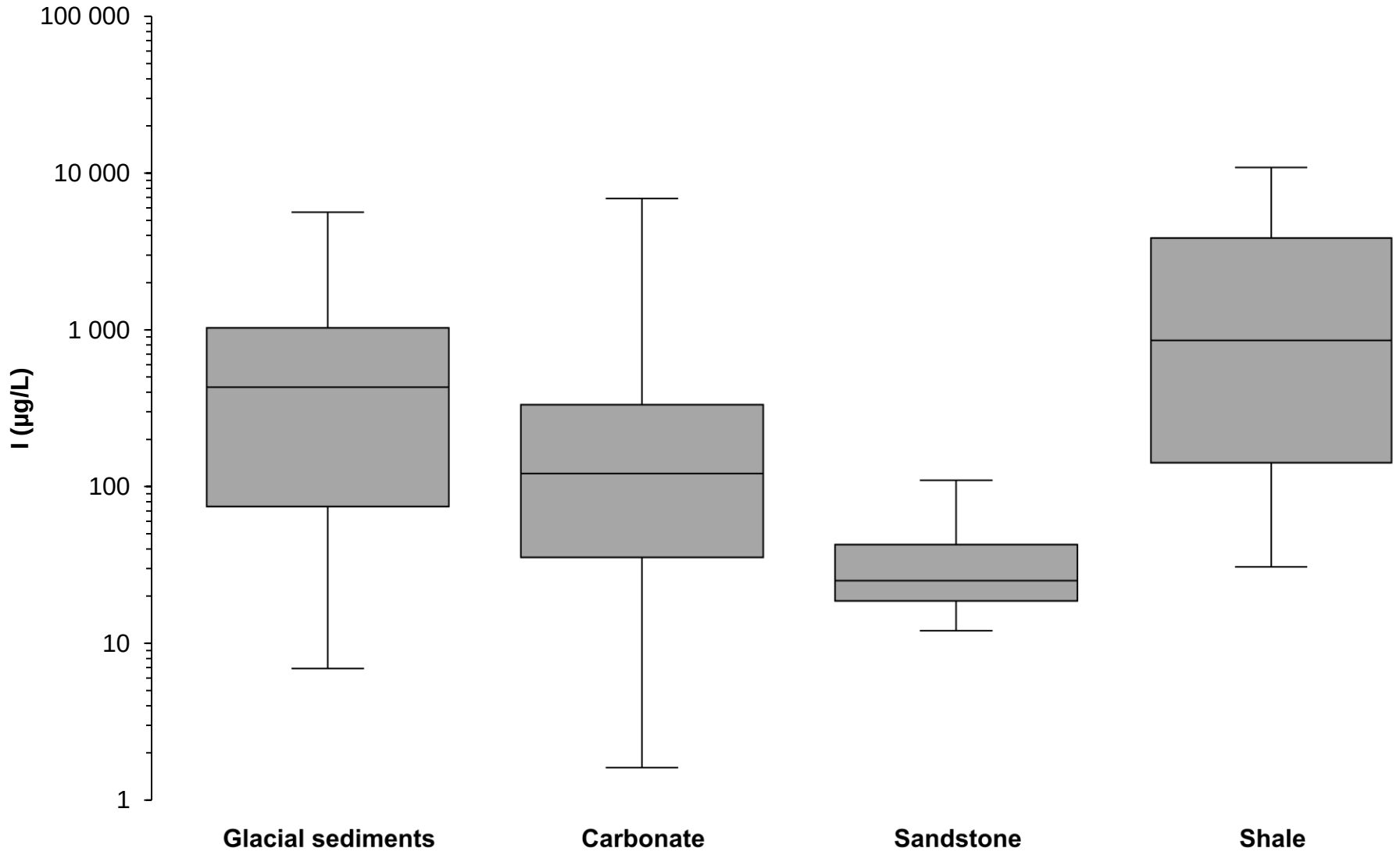
100 000
10 000
1 000
100
10
1
I (µg/L)
Glacial sediments
Carbonate
Sandstone
Shale

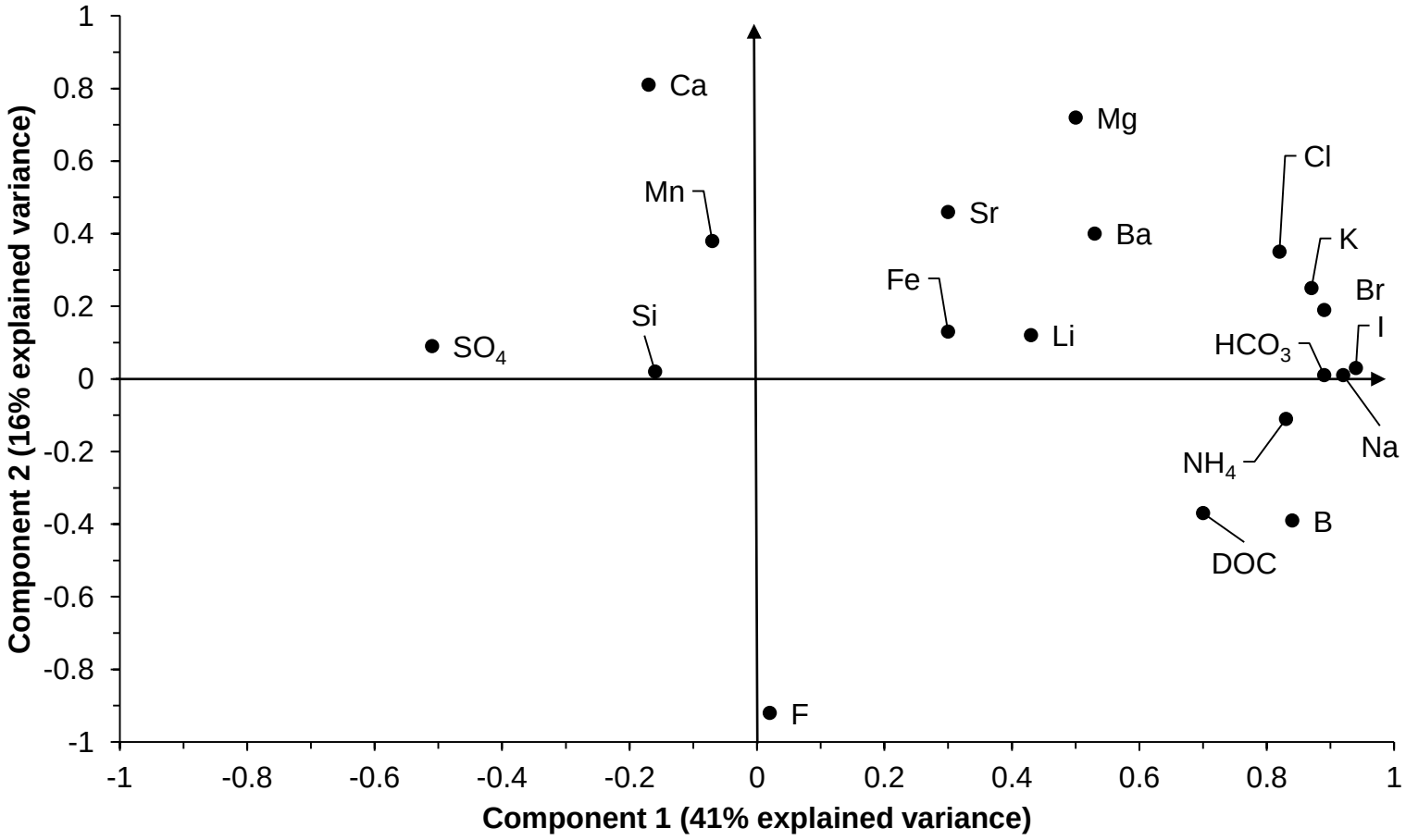
Component 2 (16% explained variance)
Component 1 (41% explained variance)
1
0.8
0.6
0.4
0.2
0
-0.2
-0.4
-0.6
-0.8
-1
-1
-0.8
-0.6
-0.4
-0.2
0
0.2
0.4
0.6
0.8
1
Ca
Mg
Cl
Mn
Sr
Ba
K
Fe
Br
Si
Li
I
SO4
HCO3
Na
NH4
B
DOC
F

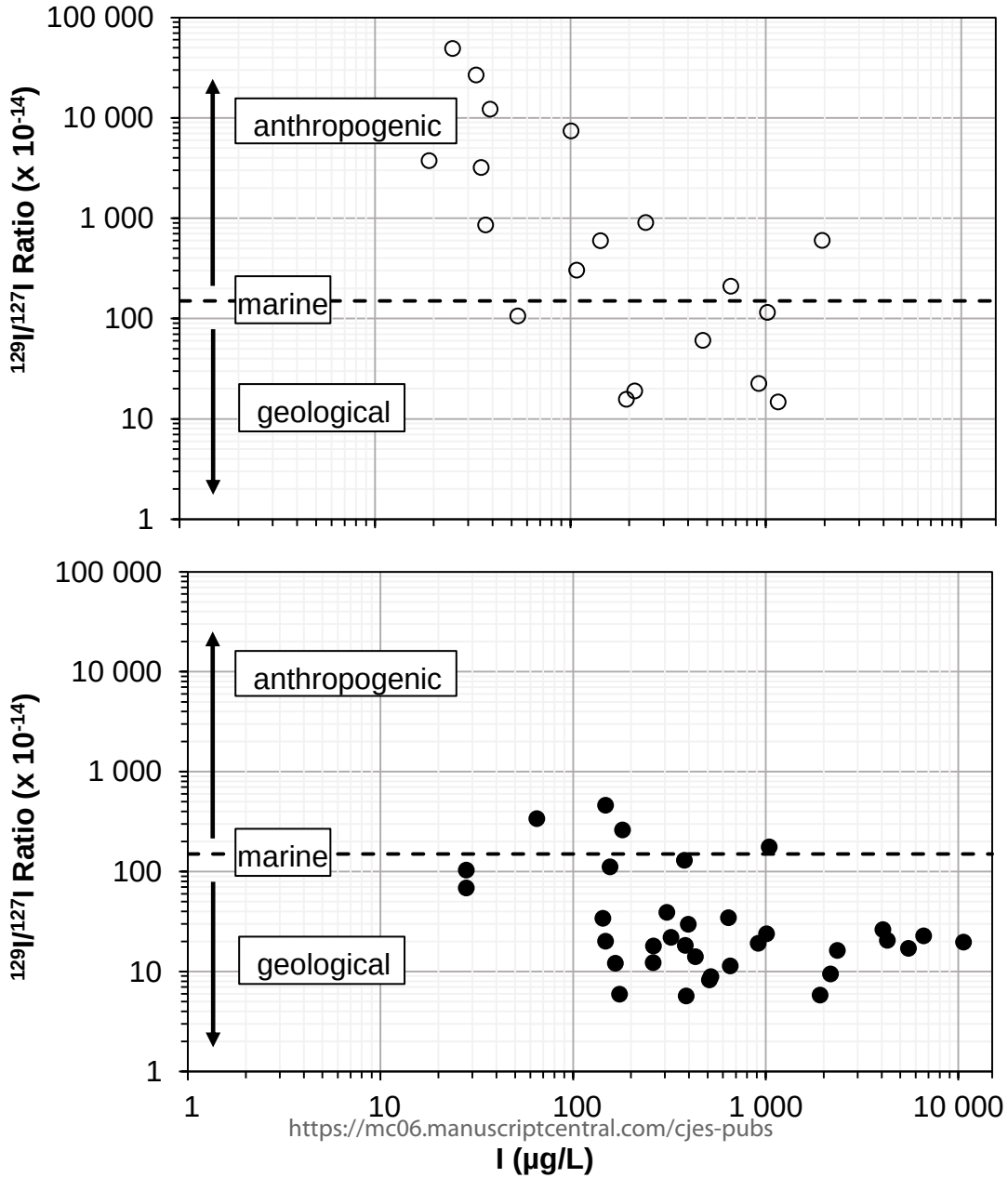
100 000
10 000
1 000
100
10
1
anthropogenic
marine
geological
$^{129}I/^{127}I$ Ratio (x 10^{-14})
100 000
10 000
1 000
100
10
1
anthropogenic
marine
geological
$^{129}I/^{127}I$ Ratio (x 10^{-14})
1
10
100
1 000
10 000
I (µg/L)

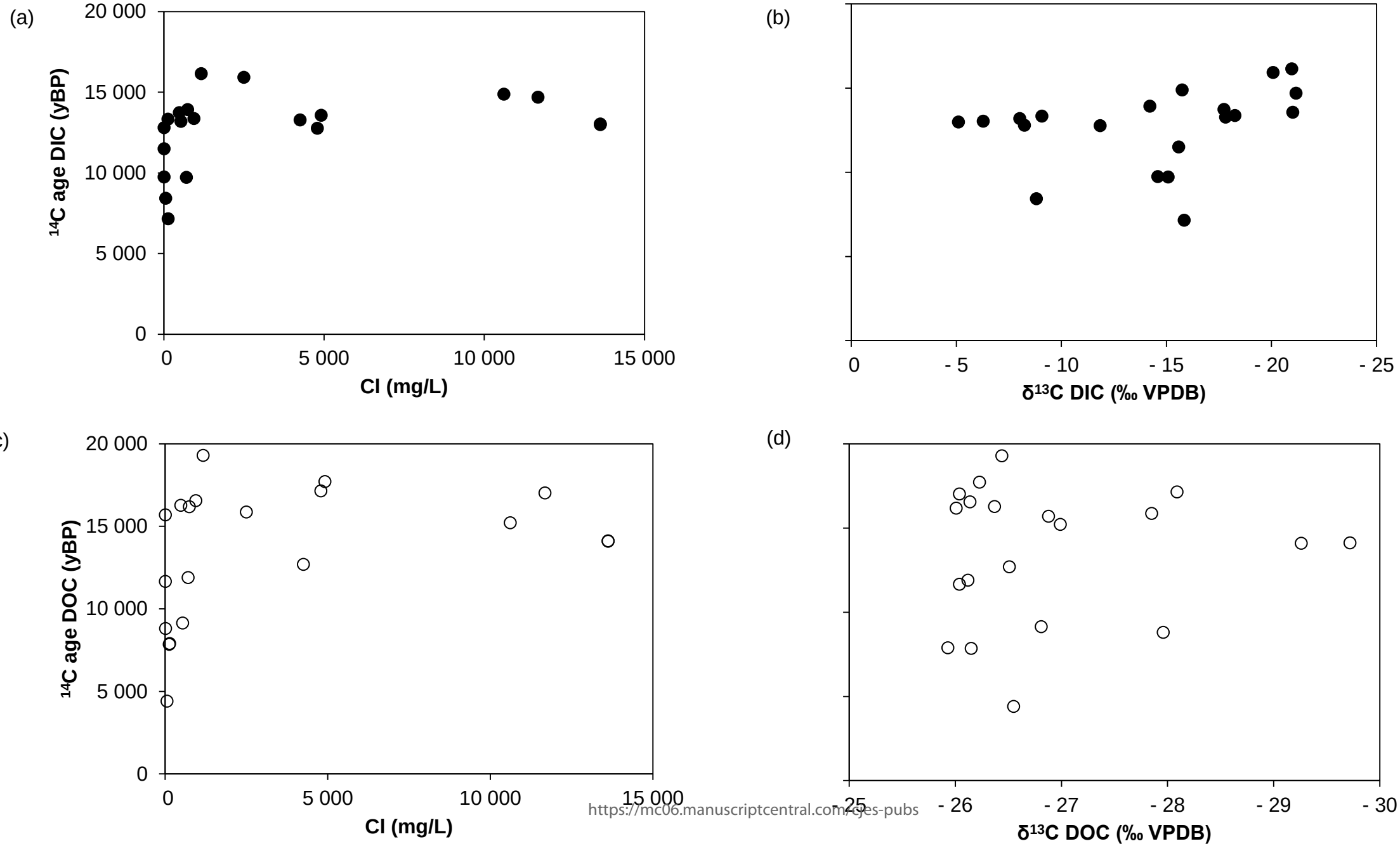
(a)
20 000
15 000
10 000
5 000
0
^{14}C age DIC (yBP)
0
5 000
10 000
15 000
Cl (mg/L)
(b)
0
- 5
- 10
- 15
- 20
- 25
δ^{13}C DIC (‰ VPDB)
(c)
20 000
15 000
10 000
5 000
0
^{14}C age DOC (yBP)
0
5 000
10 000
15 000
Cl (mg/L)
(d)
- 25
- 26
- 27
- 28
- 29
- 30
δ^{13}C DOC (‰ VPDB)

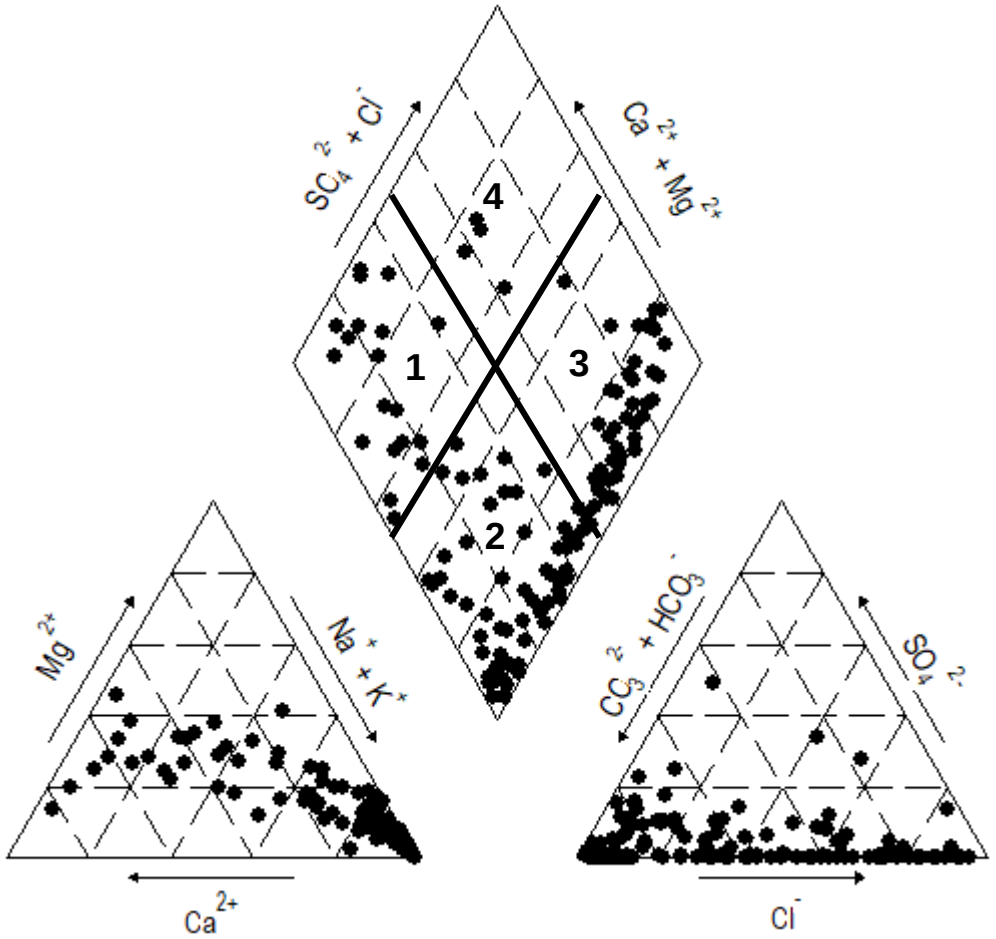
$SO_4^{2-} + Cl^-$
$Ca^{2+} + Mg^{2+}$
1
2
3
4
Mg^{2+}
$Na^+ + K^+$
Ca^{2+}
$CO_3^{2-} + HCO_3^-$
SO_4^{2-}
Cl^-

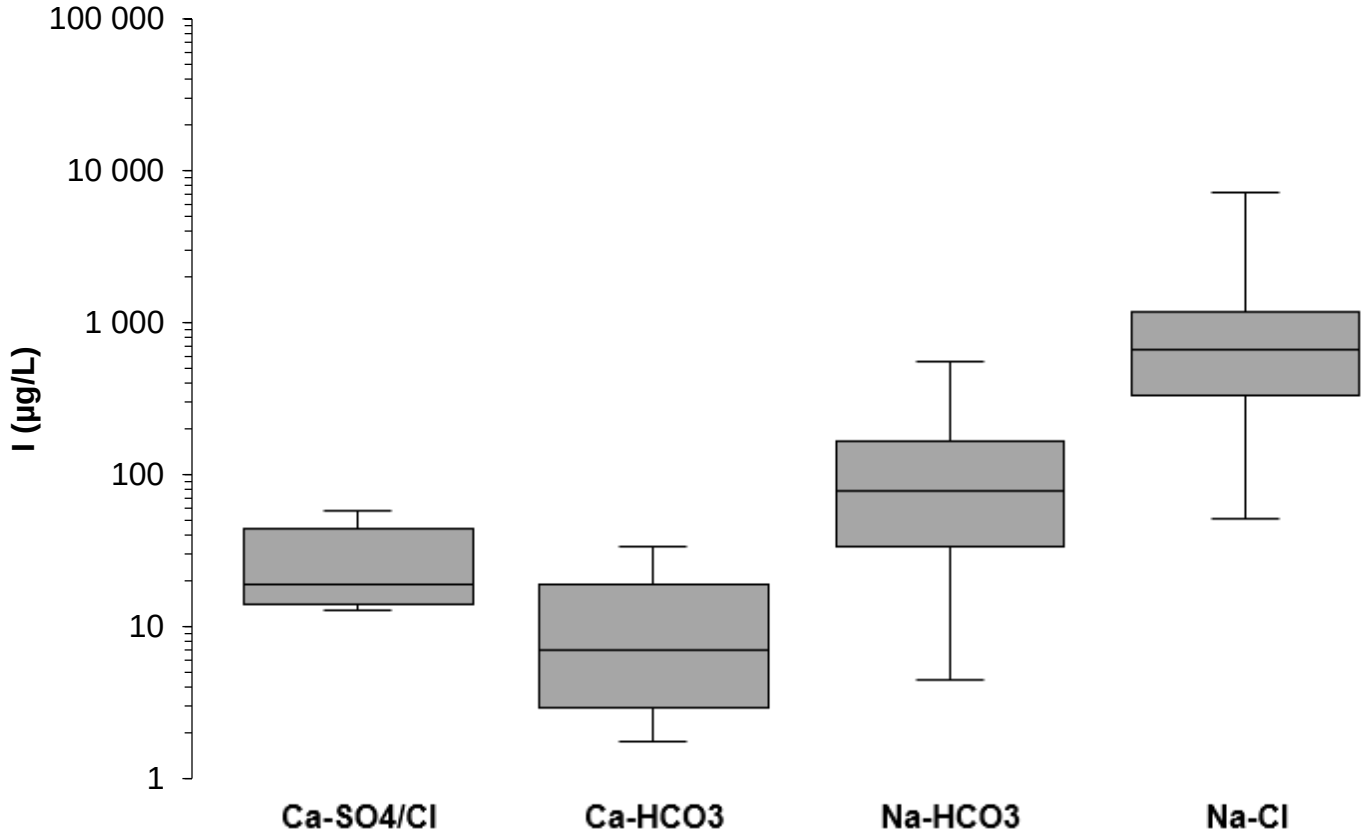
100 000
10 000
1 000
100
10
1
I (µg/L)
Ca-SO4/Cl
Ca-HCO3
Na-HCO3
Na-Cl

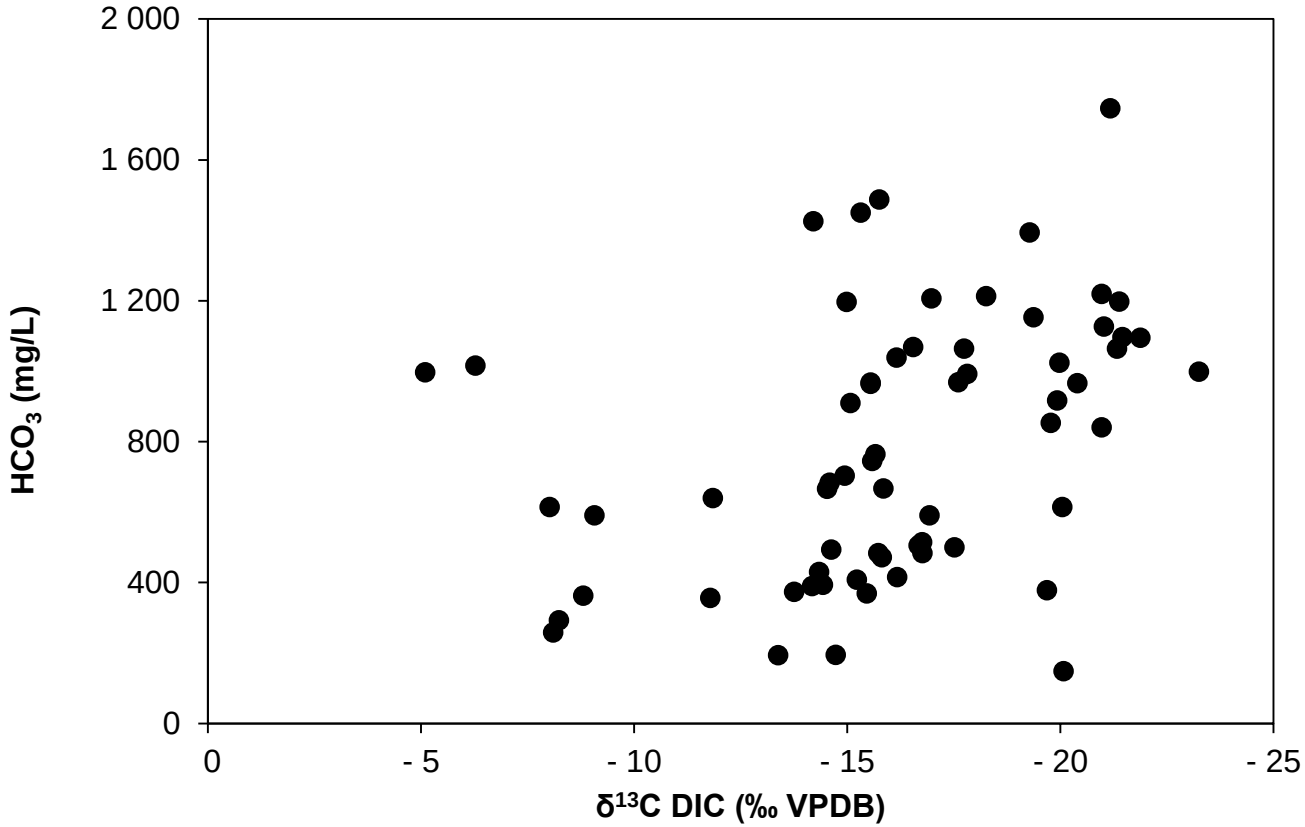
2 000
1 600
1 200
800
400
0
HCO_3 (mg/L)
0
- 5
- 10
- 15
- 20
- 25
$\delta^{13}C$ DIC (‰ VPDB)